Chapter 4

Optimization of annular fin array

This chapter presents a simultaneous optimization procedure optimizing various fin array related performance parameter. The objective functions are designed taking into account the three important factors, the heat transfer rate, the total fin volume and the maximum thermal stress developed. A set of constraints related to geometric parameter of the fin array configuration consisting of a number of identical fins are imposed. Design variables in the optimization problem are parameter related to profile of an individual fin and total number of fins in the array.

The variation of thermal conductivity k with temperature T_i given by Eq. (3.1) is also adopted here for the analysis of annular fin array.

For air flowing through two consecutive fins, the average natural convective heat transfer coefficient (h) can be estimated by the correlation expressed by Eq. (4.1) [78] with s_m being the mean fin inter-spacing and Ra the Rayleigh number in the laminar range of $5 \leqslant Ra \leqslant 10^8$ with properties evaluated at the film temperature of $\frac{T_b + T_\infty}{2}$.

$$
\left.
\begin{aligned}
h &= \frac{k}{s_m} \left\{ c_0 + c_1 Ra^{a_0} \left(\frac{r_o}{r_b} \right)^{a_1} + c_2 Ra^{a_2} + c_3 \left(\frac{r_o}{r_b} \right)^{a_3} \right\} \\
\text{where,} \quad Ra &= \frac{g \beta_e (T_b - T_\infty) s_m^4}{2 \nu_s \alpha_s r_o} \\
c_0 &= -3.827 \ ; \quad c_1 = 0.047 \ ; \quad c_2 = 1.039 \ ; \quad c_3 = 2.548 \\
a_0 &= 0.348 \ ; \quad a_1 = 0.173 \ ; \quad a_2 = 0.175 \ ; \quad a_3 = 0.009
\end{aligned}
\right\}
\quad (4.1)
$$

It is to be mentioned that the correlation given by Eq. (4.1) was proposed by Senapati et al. [78] for uniform thickness annular fin array. Since no such correlation for an annular stepped or continuously varying thickness fin array could be found in specialized literature, it is adopted here considering s_m being the mean fin inter-spacing.

The thickness of a fin is considered to be very small, so that the temperature difference in its lateral direction would become negligible and the flow of heat through the fin can be treated as one-dimensional. Since the heat transfer by radiation can be neglected for a low temperature difference [53], the heat loss from the fin surface as well as from the fin inter-spacing is considered to be taken place by natural convection only. Steady state heat transfer without internal heat generation is made another assumption. Moreover, the fin array is taken in the horizontal orientation so as to make the gravity forces parallel to the fins. Considering the temperature at the base of the fins, T_b as constant, the steady state analysis for the studied fin arrays based on Eq. (3.1) are discussed as follows:

4.1   Stepped fin array

An annular fin array consisting of identical fins with two-stepped rectangular cross-sectional area, which is attached to a heat exchanger of cylindrical primary surface with uniform fin inter-spacing is taken up for analyses.

The schematic diagram of such an annular fin array is shown Fig. 4.1(a). In Fig. 4.1(a), r_b and r_o are respectively the inner and outer radii of a fin with r_1 as the radius at its point of step change in thickness, t_1 and t_2 are respectively the cross-sectional half-thickness at the base and tip of the fin, s_b is the fin inter-spacing at the base, W is the total length of the primary surface, and n_{fin} is the number of fins in the fin array.

Note in Fig. 4.1(a) that the attachment of the fin array on the primary surface is

(a) Schematic diagram of the fin array.

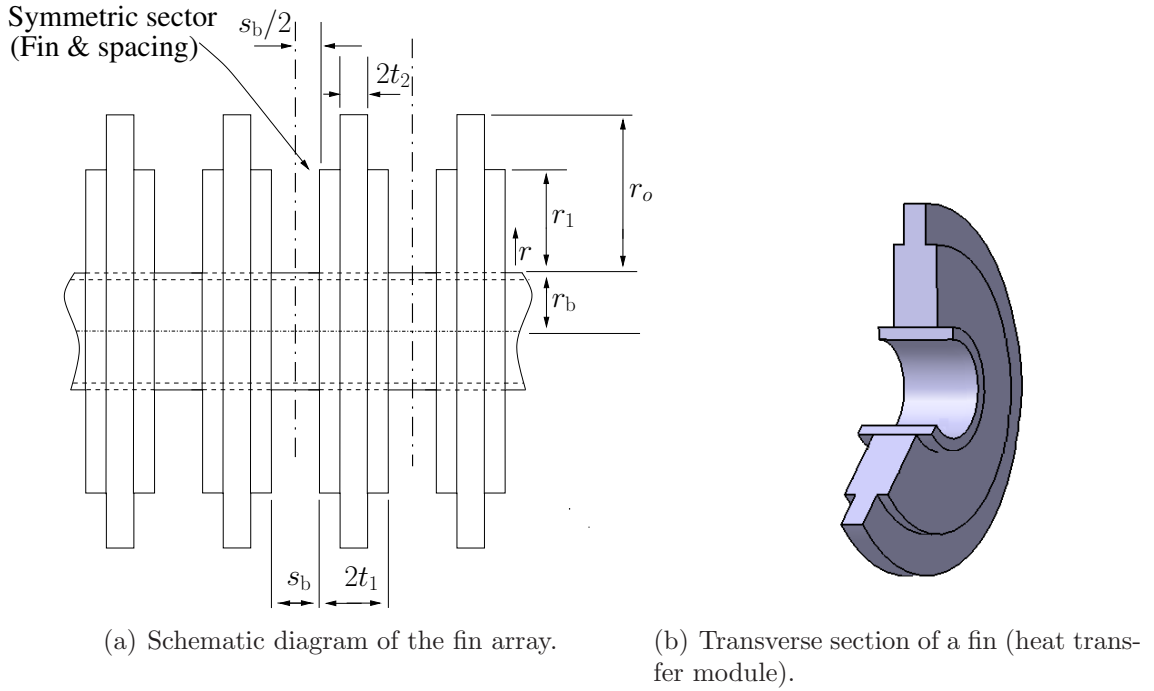(b) Transverse section of a fin (heat transfer module).

Figure 4.1: Array of annular stepped fins.

actually a repetitive surface containing one fin and some spacing (fin inter-spacing). Hence, the thermal analysis of the whole fin assembly can be done by analyzing a repetitive symmetric sector (heat transfer module) only. A schematic diagram of such a module is shown in Fig. 4.1(b).

4.1.1 Formulation for heat transfer equation

Having Eqs. (3.1) and (4.1), the steady state energy balance governing equation for an individual fin of the fin array can be expressed by Eq. (4.2).

$$\left.\begin{array}{l} \frac{d}{dr}\left[r\left\{1+\beta\left(T_i-T_\infty\right)\right\}\frac{dT_i}{dr}\right]-\frac{hr}{k_a t_i}\left(T_i-T_\infty\right)=0 \\[2mm] \text{where,} \quad r_b \leq r \leq r_1 ; \quad \text{for} \quad i=1 \\[2mm] \qquad\qquad r_1 \leq r \leq r_o ; \quad \text{for} \quad i=2 \end{array}\right\} \qquad (4.2)$$

In this study, it is considered that the temperature at the base of a fin (i.e., T_b) is constant and heat is transferred from the tip of the fin to the surrounding by natural convection only. Also, there must be a continuity of temperature as well as

energy balance at the interface of the two steps of a fin. Hence, Eq. (4.2) will be subjected to the boundary conditions given by Eq. (4.3).

$$T_1 = \begin{cases} T_{\mathrm{b}} \ ; & \text{if} \quad r = r_{\mathrm{b}} \\ T_2 \ ; & \text{if} \quad r = r_1 \end{cases} \tag{4.3a}$$

$$-k_{\mathrm{a}} \left\{ 1 + \beta \left(T_2 - T_\infty \right) \right\} \frac{dT_2}{dr} = h \left(T_2 - T_\infty \right) \ ; \quad \text{at} \quad r = r_o \tag{4.3b}$$

$$-t_1 k_{\mathrm{a}} \left\{ 1 + \beta \left(T_1 - T_\infty \right) \right\} \frac{dT_1}{dr} = -t_2 k_{\mathrm{a}} \left\{ 1 + \beta \left(T_2 - T_\infty \right) \right\} \frac{dT_2}{dr}$$
$$+ h_s \left(t_1 - t_2 \right) \left(T_1 - T_\infty \right) \ ; \quad \text{at} \quad r = r_1 \tag{4.3c}$$

In order to normalize the temperature distribution and fin dimensions shown in Fig. 4.1(a), some non-dimensional parameters are defined as given by Eq. (4.4).

$$\left. \begin{array}{llll} R_1 = \frac{r_{\mathrm{b}}}{r_o} & R_o = \frac{r_1}{r_o} & R = \frac{r}{r_o} \\[2mm] y_s = \frac{t_2}{t_1} & \xi = \frac{t_1}{r_{\mathrm{b}}} & \mathrm{Bi} = \frac{h r_{\mathrm{b}}}{k_{\mathrm{a}}} \\[2mm] \theta = \frac{T_1 - T_\infty}{T_{\mathrm{b}} - T_\infty} & \phi = \frac{T_2 - T_\infty}{T_{\mathrm{b}} - T_\infty} & \delta = \frac{T_\infty}{T_{\mathrm{b}} - T_\infty} & \alpha = \left(T_{\mathrm{b}} - T_\infty \right) \beta \end{array} \right\} \tag{4.4}$$

Finally, in terms of the non-dimensional parameters of Eq. (4.4), the thermal model governing Eqs. (4.2) and (4.3) are normalized in dimensionless forms as expressed by Eqs. (4.5) and (4.6).

$$\left. \begin{array}{l} (1 + \alpha\kappa)\frac{d^2\kappa}{dR^2} + \left\{ \alpha\frac{d\kappa}{dR} + \frac{1}{R}(1 + \alpha\kappa) \right\} \frac{d\kappa}{dR} - Z^2\kappa = 0 \\[2mm] \text{where,} \quad \kappa = \theta \ , \ Z = \frac{Z_0}{R_1} \ ; \quad \text{if} \quad R_1 \le R \le R_o \\[2mm] \qquad\qquad \kappa = \phi \ , \ Z = \frac{Z_1}{\sqrt{y_s}} \ ; \quad \text{if} \quad R_o \le R \le 1 \\[2mm] \qquad Z_0 = \sqrt{\frac{\mathrm{Bi}}{\xi}} \\[2mm] \qquad Z_1 = \frac{Z_0}{R_1} \end{array} \right\} \tag{4.5}$$

$$\theta = \begin{cases} 1 \ ; & \text{at} \quad R = R_1 \\ \phi \ ; & \text{at} \quad R = R_o \end{cases} \tag{4.6a}$$

$$-\left(1 + \alpha\phi\right)\frac{d\phi}{dR} = \frac{\text{Bi}}{R_1}\phi \ ; \qquad\qquad\qquad\qquad \text{at} \quad R = 1 \tag{4.6b}$$

$$R_1\left(1 + \alpha\theta\right)\frac{d\theta}{dR} = y_s R_1\left(1 + \alpha\phi\right)\frac{d\phi}{dR} - \text{B}i\left(1 - y_s\right)\theta \ ; \quad \text{at} \quad R = R_o \tag{4.6c}$$

4.1.2 Optimization modeling

In the present study, the performance of the annular fin array having fins of step profile is evaluated in different combination of the four parameters, which are the total heat transfer rate from the fin array (f_1), total fin volume (f_2), surface efficiency (f_3) and augmentation factor (f_4) of the fin array. The configuration of the fin array as shown in Fig. 4.1(a) can be defined in terms of five independent parameters, which are the radius of an individual fin at the point of step change in thickness (r_1), outer radius of the fin (r_o), cross-sectional half thickness of the thick (first) step of the fin (t_1), cross-sectional half thickness of the thin (second) step of the fin (t_2) and the total number of fins in the fin array (n_{fin}). Any change in the values of any of these five independent parameters will give rise to a new fin array configuration with new values of the four functions considered for measuring the performance of the array. Hence, the present problem at hand can be formulated as a multi-objective optimization problem as expressed by Eq. (4.7) by treating the five independent parameters as the design variables and the four performance

parameters as the objective functions.

$$
\left.
\begin{aligned}
\text{Determine} \qquad & \boldsymbol{x} \; \equiv \; (r_1, r_o, t_1, t_2, n_{\text{fin}})^{\mathrm{T}} \\
\text{to maximize} \qquad & \boldsymbol{z}(\boldsymbol{x}) \; \equiv \; \{f_1(\boldsymbol{x}), f_3(\boldsymbol{x}), f_4(\boldsymbol{x})\} \\
\text{minimize} \qquad & \boldsymbol{f}(\boldsymbol{x}) \; \equiv \; \{f_2(\boldsymbol{x})\} \\
\text{subject to} \qquad & g_1(\boldsymbol{x}) \; \equiv \; r_1 > r_{\text{b}} \\
& g_2(\boldsymbol{x}) \; \equiv \; r_o > r_1 \\
& g_3(\boldsymbol{x}) \; \equiv \; t_1 \leqslant \frac{W}{4} \\
& g_4(\boldsymbol{x}) \; \equiv \; t_1 > t_2 \\
& g_5(\boldsymbol{x}) \; \equiv \; \left\lceil \frac{W}{2t_1 + s_{\max}} \right\rceil \leqslant n_{\text{fin}} \leqslant \left\lfloor \frac{W}{2t_1 + s_{\min}} \right\rfloor \\
& r_1, r_o, t_1, t_2 \geq 0 \; .
\end{aligned}
\right\}
\qquad (4.7)
$$

In Eq. (4.7), constraints $g_1(\boldsymbol{x})$, $g_2(\boldsymbol{x})$ and $g_4(\boldsymbol{x})$ are related to the geometry of the individual fins, while constraints $g_3(\boldsymbol{x})$ and $g_5(\boldsymbol{x})$ are related to the configuration of the fin array. Constraint $g_1(\boldsymbol{x})$ ensures the existence of the fins by making the radius at step change in thickness (r_1) greater than the predefined radius at the base (r_{b}), and constraint $g_2(\boldsymbol{x})$ ensures the existence of two steps in a fin by making the outer radius (r_o) greater than radius at step change in thickness (r_1) while constraint $g_4(\boldsymbol{x})$ ensures that the inner step of the fin is thicker than its outer step. On the other hand, constraint $g_3(\boldsymbol{x})$ restricts the fin half-thickness at the base (t_1) to such a value that an array of fins can be formed by accommodating at least two fins within the limited predefined length (W) of the primary surface, and constraint $g_5(\boldsymbol{x})$ forms the fin array with the lower limit for two fins and the upper limit avoiding the excess number of fins over the length (W) of the primary surface (($s_{\min}, s_{\max}$) is the allowable range of fin inter-spacing at base). The last line in Eq. (4.7) makes the design variable non-negative.

The maximization of the heat transfer rate, $f_1(\boldsymbol{x})$, surface efficiency, $f_3(\boldsymbol{x})$ and augmentation factor, $f_4(\boldsymbol{x})$ would enhance the overall thermal performance of the fin array, while the minimization of the total fin volume, $f_2(\boldsymbol{x})$ of the array will reduce the fin material cost. These objective functions, in terms of the notations and formulations of the thermal model of the fin array presented in Section 4.1.1,

can be expressed by Eq. (4.8).

$$f_1(\boldsymbol{x}) = n_{\text{fin}} \times \left\{ -kA_{\text{b}} \left.\frac{dT_1}{dr}\right|_{r=r_{\text{b}}} + hA_{\text{sp}}(T_{\text{b}} - T_\infty) \right\} \tag{4.8a}$$

$$f_2(\boldsymbol{x}) = n_{\text{fin}} \times 2\pi \left\{ t_1 \left(r_1^2 - r_{\text{b}}^2\right) + t_2 \left(r_o^2 - r_1^2\right) \right\} \tag{4.8b}$$

$$f_3(\boldsymbol{x}) = \frac{1}{n_{\text{fin}}} \times \frac{f_1(\boldsymbol{x})}{hA_{\text{s}}(T_{\text{b}} - T_\infty) + hA_{\text{sp}}(T_{\text{b}} - T_\infty)} \tag{4.8c}$$

$$f_4(\boldsymbol{x}) = \frac{1}{n_{\text{fin}}} \times \frac{f_1(\boldsymbol{x})}{hA_{\text{b}}(T_{\text{b}} - T_\infty) + hA_{\text{sp}}(T_{\text{b}} - T_\infty)} \tag{4.8d}$$

where, $\quad A_{\text{b}} = 4\pi r_{\text{b}} t_1$

$$A_s = 2\pi \left(r_o^2 - r_{\text{b}}^2\right) + 4\pi \left\{ r_1 (t_1 - t_2) + r_o t_2 \right\} \tag{4.8e}$$

$$A_{sp} = 2\pi r_{\text{b}} s_{\text{b}}$$

4.1.3   Solution procedure

The multi-objective optimization model of the fin array design problem, formulated in Eq. (4.7), is solved by using the non dominated sorting genetic algorithm II (NSGA-II).

4.1.3.1   Constraints handling through variable bounds

Though the design of the studied fin array is formulated in Eq. (4.7) as a constrained optimization problem, it can easily be handled as an unconstrained optimization problem.

Since r_{b} (radius of a fin at its base) is a predefined fixed parameter, constraints $g_1(\boldsymbol{x})$ and $g_2(\boldsymbol{x})$ can be made satisfied by generating two values in the range of $(r_{\text{b}}, r_{\text{max}}]$ and then sorting them in ascending order as the values of r_1 (radius at step change in thickness) and r_o (outer radius of the fin), respectively (r_{max} is the allowable upper limit of r_1 and r_o). Similarly, constraints $g_3(\boldsymbol{x})$ and $g_4(\boldsymbol{x})$ can be

made satisfied by generating two values in the range of $\left[t_{\min}, \frac{W}{4}\right]$ and then sorting them in descending order as the values of t_1 (fin half-thickness at the base) and t_2 (fin half-thickness at the tip), respectively ($t_{\min}$ is the allowable lower limit of t_1 and t_2). Note that the maximum half-thickness of a fin could be $\frac{W}{4}$, but it may be taken to be $t_{\max} \ll \frac{W}{4}$ if the heat flow through the fin is to be treated as one-dimensional.

The process for satisfying constraint $g_5(\boldsymbol{x})$ is slightly different. In this case, the range $[s_{\min}, s_{\max}]$ for the fin inter-spacing at the base is to be so chosen that the air flowing through two consecutive fins would maintain the Rayleigh number in the laminar range of $[5, 10^8]$. Accordingly, the range $[s_{\min}, s_{\max}]$ may be obtained through a reserve calculation. Since the Rayleigh number (Ra) as expressed in Eq. (4.1) is a function only of the fin mean inter-spacing (s_m) and the fin outer radius (r_o) keeping all other terms constant for a given scenario, s_m can be computed as $s_{\min}$ by replacing r_o by $r_{\max}$ and Ra by its lower limit of 5. Similarly, s_m can be computed as $s'_{\max}$ (maximum fin inter-spacing at the tip) by replacing r_o by $r_{\min}$ ($r_{\min}$ ($r_{\min} > r_b$) is the allowable minimum value of r_o) and Ra by its upper limit of 10^8, and then to estimate $s_{\max}$ by deducting $2(t_{\max} - t_{\min})$ from $s'_{\max}$.

Once all the five constraints are made satisfied automatically as above, the equal fin inter-spacing (s_b) at base for all the adjacent pairs of fins can be obtained using Eq. (4.9).

$$s_b = \frac{W}{n_{\text{fin}}} - 2t_1 \ .\tag{4.9}$$

4.1.3.2   Evaluation of objective functions

In every iteration of the employed optimizer, the values of the four objective functions given by Eqs. (4.8a)–(4.8d) will be required, which are to be evaluated numerically. The critical one is the heat transfer rate, f_1 given by Eq. (4.8a), which is to be evaluated by solving the problem governing Eq. (4.5) along with its boundary conditions given by Eq. (4.6). For this, the hybrid spline difference method (HSDM) is used. The results of HSDM for annular step fin are already validated with published exact results in Section 3.1.3. The HSDM method is based on a discretization

scheme as given in Eq. (A.9).

The following is the detail procedure for evaluating f_1 through the HSDM scheme expressed by Eq. (A.9):

(a) Discretize Eqs. (4.5) and (4.6) using Eq. (A.9).

(b) Evaluate p_n ($n = 0, 1, \ldots, N$) by solving the discretized forms of Eqs. (4.5) and (4.6), which can be done through the variant of the Thomas algorithm proposed by Martin and Boyd [64].

(c) At all the grid points, evaluate the dimensionless temperature distribution and their derivatives up to the second order (i.e., θ_n, ϕ_n, θ'_n, ϕ'_n, θ''_n and ϕ''_n) using the values of p_n in Eq. (A.9).

(d) Evaluate the temperature gradient at the base of the fin, i.e., $\frac{dT_1}{dr}\big|_{r=r_{\mathrm{b}}}$, using the dimensionless temperature gradient θ'_o at the base of the fin.

(e) Finally, evaluate the heat transfer rate from the fin array using the value of $\frac{dT}{dr}\big|_{r=r_{\mathrm{b}}}$ in Eq. (4.8a).

4.1.4   Numerical experimentation and discussion

An annular fin array with identical fins of rectangular cross-section having a step change in thickness is taken up in the present study. It is assumed that the temperature at the base of the fins is constant, thermal conductivity of the fin material varies linearly with temperature, and heat is dissipated from the fin array by natural convection only.

The operating condition, the thermal properties of the fin material, and the fin array configuration with reference to Fig. 4.1(a), considered for numerical experimentation, are listed in Table 4.1, while the opted user-defined algorithmic parameter settings for NSGA-II (the applied optimizer) are given in Table 3.3. With those input parameters, NSGA-II is applied to Eq. (4.7) for studying the problem at hand

Table 4.1: Operating conditions, fin material properties, and fin array geometry for stepped fin array.

Parameter	Value/ range of value
Ambient temperature, T_∞	300 K
Fin temperature at the base, $T_{\rm b}$	373 K
Thermal conductivity of the fin material at T_∞, $k_{\rm a}$	186 W/mK
Parameter for variable thermal conductivity, β	-0.00018 K^{-1}
Fin base radius, $r_{\rm b}$	2.0 cm
Outer radii of two steps of a fin, $[r_{\min}, r_{\max}]$ for r_1 and r_o	[2.5–6.0] cm
Half-thickness of two steps of a fin, $[t_{\min}, t_{\max}]$ for t_1 and t_2	[0.01–0.2] cm
Length of the primary cylinder, W	40.0 cm
Fin inter-spacing at base, $[s_{\min}, s_{\max}]$	[0.36, 18.0] cm

under two scenarios. In the first scenario, the objective functions f_1–f_4 given by Eq. (4.8) are optimized in different pairs, while all the four objective functions are optimized simultaneously in the second scenario.

4.1.4.1 Scenario I

At the first instance, the fin array design problem is studied for maximizing the total heat dissipation rate (f_1) from the fin array and simultaneously minimizing the total fin volume (f_2) of the array. Fig. 4.2(a) shows the obtained Pareto optimal front

(a) Pareto front in terms of f_1 and f_2.   (b) Pareto front in terms of f_1 and f_3.
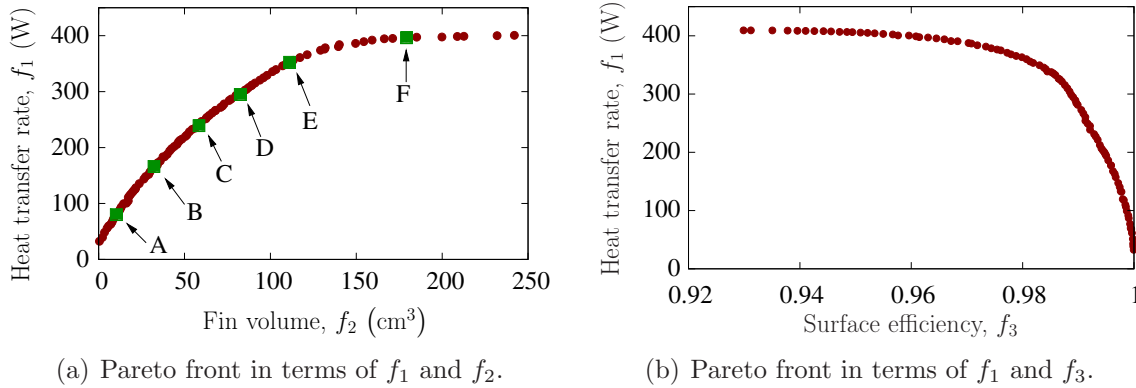
Figure 4.2: Pareto fronts of f_1 separately paired with f_2 and f_3.

containing a set of trade-off solutions in terms of f_1 and f_2, which clearly depicts the conflicting nature between the two objective functions. The efficient fin geometries corresponding to six selective trade-off solutions marked by A–F in Fig. 4.2(a) are shown in Fig. 4.3, where the variations in the pattern of the individual fins and the total number of fins in the fin array are most noticeable. Apart from the optimum values of the five design variables (r_1, r_o, t_1, t_2 and $n_{\rm fin}$) and optimized two objective
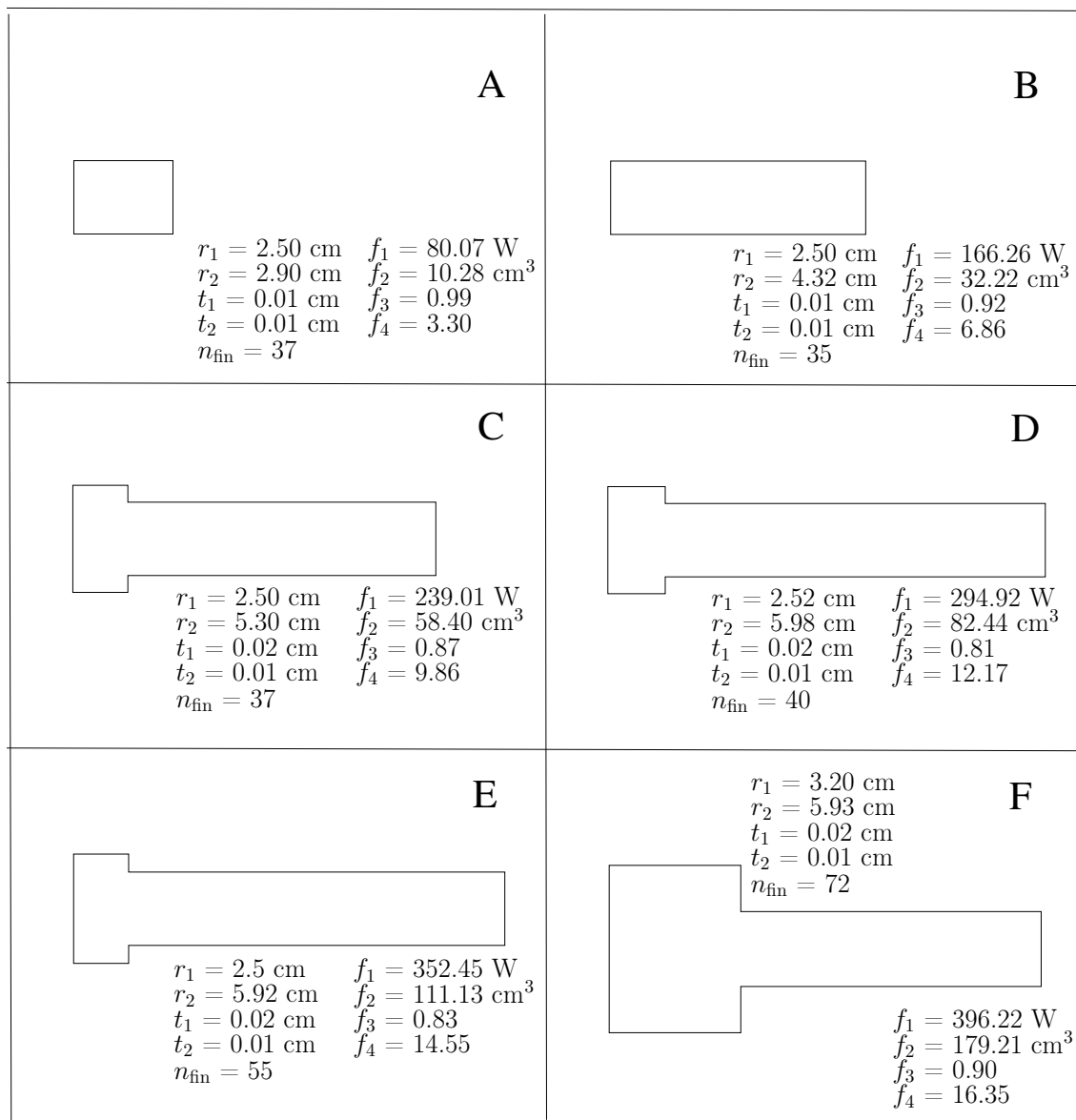
Figure 4.3: Selective efficient fin geometries (corresponding to trade-off solutions A–F of Fig. 4.2(a).)

functions (f_1 and f_2), the corresponding values of the surface efficiency (f_3) and augmentation factor (f_4) are also computed and shown in Fig. 4.3.

Notice in Fig. 4.3 that the pattern of variation of f_3 with respect to those of f_1 and f_2 is not very clear. Hence, the fin array design problem is studied in the second step for maximizing the heat dissipation rate f_1 from the fin array and simultaneously maximizing the surface efficiency f_3 of the fin array. The obtained Pareto front is shown in Fig. 4.2(b), where it is seen that f_1 conflicts with f_3 also, i.e., an improvement in f_1 degrades f_3 by some amount and *vice-versa*.

Computing the augmentation factor values of the trade-off solutions of the Pareto front of Fig. 4.2(b), they are plotted against the surface efficiency values. The plot shown separately in Fig. 4.4, where the surface efficiency and augmenta-
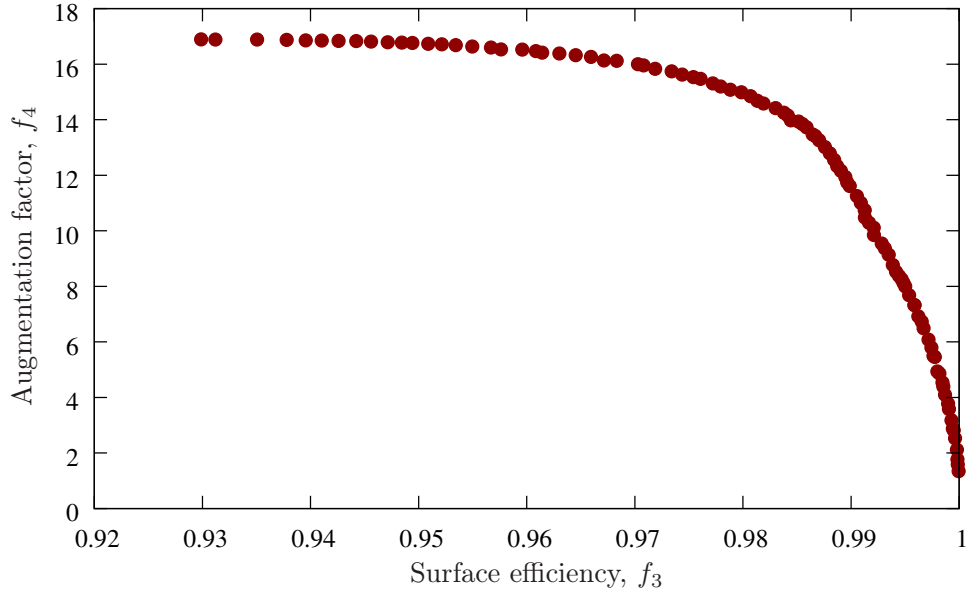

Figure 4.4: Surface efficiency and augmentation factor (of the trade-off solutions of Fig. 4.2(b).)

tion factor is found conflicting with each other, i.e., an increase in the augmentation factor decreases the efficiency of utilization of the fin material. Note that the surface efficiency of the fin array is the ratio of the actual heat transfer rate from the fin array to the heat transfer rate when all the surfaces of the fin array is at the base temperature, while the augmentation factor of the fin array is the ratio of the actual heat transfer rate from the fin array to the heat transfer rate from the base surface of the fin array when there are no fins.

4.1.4.2 Scenario II

In Section 4.1.4.1, studying the considered four objectives functions of the problem at hand in pairs, it is observed that their variations are arbitrary leading to no common pattern of the heat transfer rate. Hence, in order to arrive at a general conclusion, all the four objective functions, i.e., f_1–f_4 given by Eq. (4.8), are optimized here simultaneously. The obtained four-dimensional Pareto front is visualized in a parallel coordinate system (refer [88]) as shown in Fig. 4.5, where the conflicting
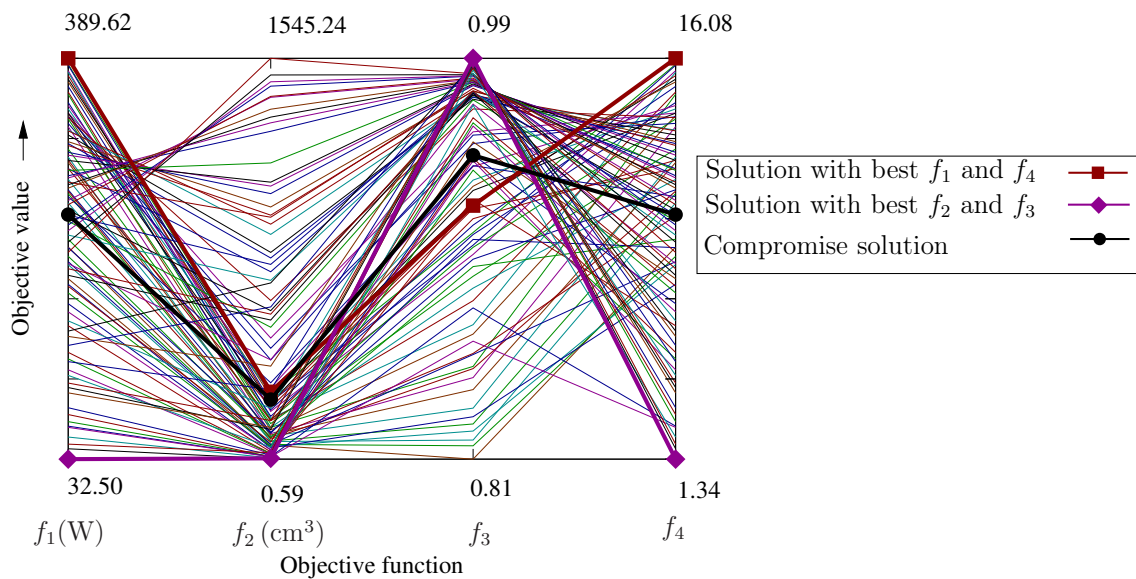
Figure 4.5: Four-dimensional Pareto in parallel coordinate system.

nature among all the optimized objective functions could be observed clearly. As an example, the solution corresponding to the highest heat transfer rate from the fin array have a moderately low fin volume and a moderately high surface efficiency, while the highest augmentation factor. With such information, it is now up to a designer to adopt suitable solution(s) based upon the availability and accessibility of resources at hand. One such compromise solution is shown in Fig. 4.5 by a thick crossing line.

4.1.5 Sensitivity analysis

In order to study the influence of the design variables on the heat transfer rate, a sensitivity analysis is performed. For this, an intermediate solution is chosen, whose various values are as follows: $r_1^\dagger = 3.35$ cm, $r_o^\dagger = 5.11$ cm, $t_1^\dagger = 0.05$ cm, $t_2^\dagger = 0.01$ cm, $n_{\text{fin}}^\dagger = 20$, $f_1^\dagger = 178.46$ W and $f_2^\dagger = 3.36$ cm^3. The problem is solved here five times, each time allowing a design variable to vary $\pm 15\%$ from the chosen value while keeping the other four design variable fixed. Fig. 4.6 shows the plots of the deviations of the heat transfer rate from the fin array against the corresponding variations in the design variables, where it is observed that the outer radius (r_o) of the fins has more influence on the heat transfer rate, followed by the number of
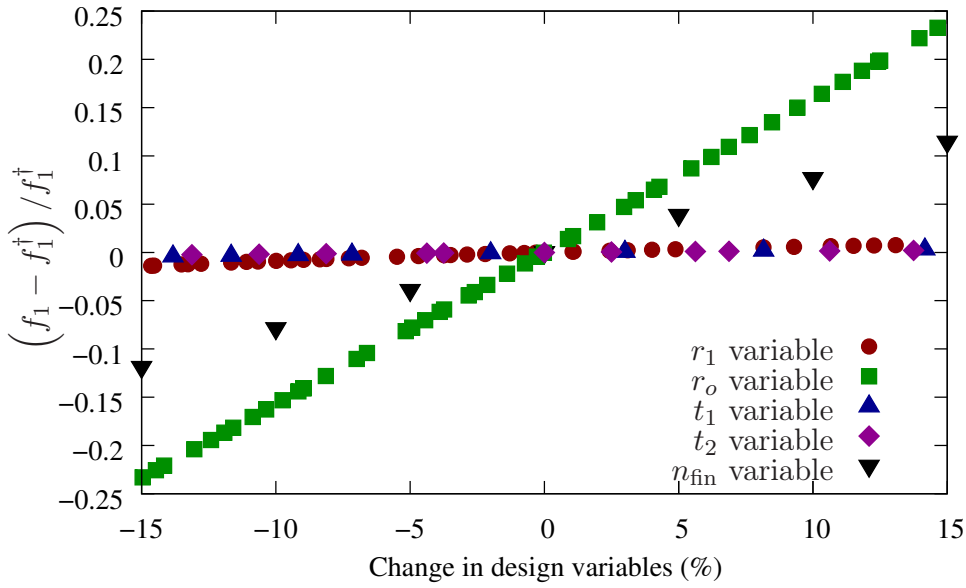
Figure 4.6: Sensitivity analysis of the heat transfer rate in terms of design variables.

fins (n_{fin}) in the fin array. On the other hand, the influences of the cross-sectional half-thickness (t_1 and t_2) and the radius of the step change in thickness (r_1) of the fins are comparatively very less. With this information at hand, a designer can adjust the design variables of the fin array in order to achieve the desired heat transfer effect based upon the availability and accessibility of information and resources.

4.2   Fin array of linearly varying thickness fins

The multi-objective optimization of an annular fin array with individual fins of linearly varying thickness, attached to a cylindrical surface, is studied here with the assumptions that Poisson's ratio, coefficient of thermal expansion, and modulus of elasticity of the fin material remain constant irrespective of any variation in temperature and the inner and outer radii of the fin are free of traction.

The schematic diagram of an array of identical annular fins, having plane fin profile and equal fin inter-spacing, is shown Fig. 4.7(a) with a centrally located circular support cylinder as the primary surface. A transverse section of a fin is also shown in Fig. 4.7(b). In Fig. 4.7(a), n_{fin} is the number of fins in the array, r_b and r_o are respectively the inner and outer radii of each fin, t is the representing

(a) Schematic diagram of the fin array.

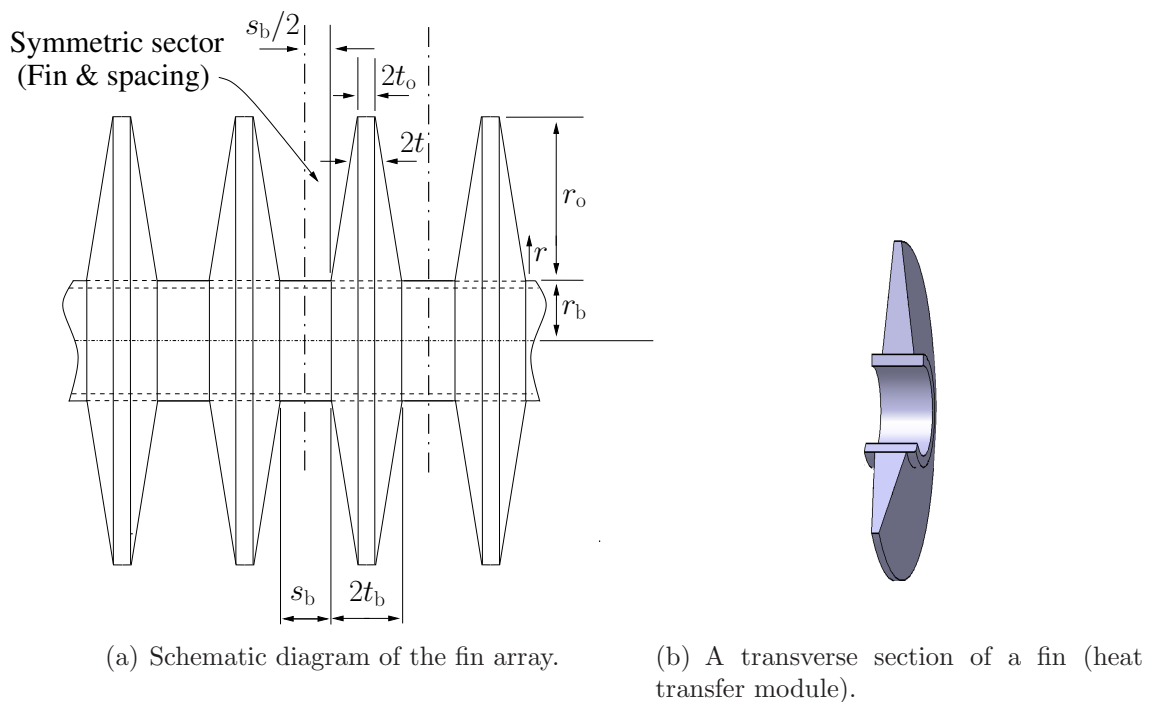(b) A transverse section of a fin (heat transfer module).

Figure 4.7: Array of annular fins having linearly varying thickness fins.

cross-sectional half thickness of a fin with t_b and t_o being its values respectively at the base and outer radius of the fin, and s_b is the inter-spacing at the base of two fins and W is the total length of the primary surface. It is to be noted that $t_o < t_b$ which will result in an array of tapered fins as shown in Fig. 4.7(a).

4.2.1 Formulation for heat transfer equation

Since a fin array is composed of a repetitive sector containing a fin and some spacing (i.e., fin inter-spacing) as shown in Fig. 4.7(b), it is considered that the thermal behavior of the entire fin array will be equivalent of that of such a repetitive sector (heat transfer module). Accordingly, the thermal model of the fin array is formulated here based on a single fin and single fin inter-spacing.

The one-dimensional energy balance (i.e., heat transfer) equation in an axisymmetric thin fin of an annular fin array under steady state condition can be given

by Eq. (4.10).

$$\frac{d}{dr}\left[rk\frac{dT}{dr}\right]t + \left[rk\frac{dT}{dr}\right]t' - hr\left(T - T_\infty\right)\left(1 + t'^2\right)^{\frac{1}{2}} = 0 \qquad (4.10)$$

Using the value of k as defined by Eq. (3.1), Eq. (4.10) can be rearranged as shown in Eq. (4.11).

$$\frac{d}{dr}\left[r\left\{1 + \beta\left(T - T_\infty\right)\right\}\frac{dT}{dr}\right] + \left[r\left\{1 + \beta\left(T - T_\infty\right)\right\}\frac{dT}{dr}\right]\frac{t'}{t}$$
$$- \frac{hr}{k_a t}\left(T - T_\infty\right)\left(1 + t'^2\right)^{\frac{1}{2}} = 0 \quad (4.11)$$

Since it is assumed that the fin base temperature (T_b) is constant and heat from the tip of the fin is dissipated by natural convection only, Eq. (4.11) would be subjected to the boundary conditions given by Eq. (4.12).

$$T = T_b \; ; \qquad\qquad \text{at} \quad r = r_b \qquad (4.12a)$$

$$-k_a\left\{1 + \beta\left(T - T_\infty\right)\right\}\frac{dT}{dr} = h\left(T - T_\infty\right) \; ; \quad \text{at} \quad r = r_o \qquad (4.12b)$$

In order to simplify the analysis, the dimensions of the fin array as well as the temperature distribution can be normalized by defining some dimensionless parameters as given by Eq. (4.13).

$$\left.\begin{array}{lll} X = \frac{r}{r_b} & X_o = \frac{r_o}{r_b} & \zeta = \frac{t_b}{r_b} \\[2mm] \delta_d = \beta T_\infty & \gamma_c = \frac{t}{t_b} & Bi = \frac{hr_b}{k_a} \\[2mm] \omega = \frac{T}{T_\infty} & \omega_b = \frac{T_b}{T_\infty} & \delta_c = \frac{\beta T_\infty}{(1 - \beta T_\infty)} \\[2mm] \gamma = \frac{hr_b^2}{t_b k_a (1 - \beta T_\infty)} & & \end{array}\right\} \qquad (4.13)$$

In terms of the dimensionless parameters defined in Eq. (4.13), Eqs. (4.11) and

(4.12) can be normalized as expressed by Eqs. (4.14) and (4.15), respectively.

$$\gamma_c \left\{ (1 + \delta_c \omega) \frac{d^2 \omega}{dX^2} + (1 + \delta_c \omega) \frac{1}{X} \frac{d\omega}{dX} + \delta_c \left(\frac{d\omega}{dX} \right)^2 \right\} + \gamma_c'(1 + \delta_c \omega) \frac{d\omega}{dX}$$
$$- \gamma(\omega - 1) \left(1 + \gamma_c'^2 \zeta^2 \right)^{\frac{1}{2}} = 0 \quad (4.14)$$

$$\omega = \omega_b; \quad \text{at} \quad X = 1 \quad (4.15\text{a})$$

$$(1 - \delta_d + \delta_d \omega) \frac{d\omega}{dX} + Bi(\omega - 1) = 0; \quad \text{at} \quad X = X_o \quad (4.15\text{b})$$

4.2.2 Formulation of the thermal stress model

The formulation of the thermal stress model of an individual fin of the fin array has already been discussed in Section 3.2.2.

4.2.3 Optimization modeling

As shown in Fig. 4.7(a), the configuration of an annular fin array of identical fins having plane profiles can be defined by four independent parameters. Three of those parameters are required to define the geometry of a fin, which are the outer radius (r_o), cross-sectional half thickness at the base (t_b) and cross-sectional half thickness at the outer radius (t_o) of the fin. The fourth parameter is the total number of fins (n_{fin}) forming the fin array. A change in the value of any of these four parameters will give rise to a new configuration of the fin array with new values of the four functions considered for measuring the performance of the array, which are the heat transfer rate (f_1) from the fin array, maximum thermal stress (f_2) developed in a fin, total volume of the fins (f_3) of the array and the surface efficiency (f_4) of the fin array.

In view of above, the design of the annular fin array of identical fins having plane profiles of tapered shape, as shown in Fig. 4.7(a), can be defined as a multi-objective optimization problem for determining r_o, t_b, t_o and n_{fin} as four design variables by simultaneously optimizing f_1, f_2, f_3 and f_4 as four objective functions. Accordingly, the optimization model can be formulated mathematically as given by Eq. (4.16).

$$
\left.
\begin{aligned}
\text{Determine} \quad & \boldsymbol{x} \;\equiv\; (r_o, t_b, t_o, n_{\mathrm{fin}})^{\mathrm{T}} \\
\text{to maximize} \quad & \boldsymbol{z}(\boldsymbol{x}) \;\equiv\; \{f_1(\boldsymbol{x}), f_4(\boldsymbol{x})\} \\
\text{minimize} \quad & \boldsymbol{f}(\boldsymbol{x}) \;\equiv\; \{f_2(\boldsymbol{x}), f_3(\boldsymbol{x})\} \\
\text{subject to} \quad & g_1(\boldsymbol{x}) \;\equiv\; r_o > r_b \\
& g_2(\boldsymbol{x}) \;\equiv\; t_b \leqslant \tfrac{W}{4} \\
& g_3(\boldsymbol{x}) \;\equiv\; t_o < t_b \\
& g_4(\boldsymbol{x}) \;\equiv\; \left\lceil \tfrac{W}{2t_b + s_{\max}} \right\rceil \leqslant n_{\mathrm{fin}} \leqslant \left\lfloor \tfrac{W}{2t_b + s_{\min}} \right\rfloor \\
& r_o, t_b, t_o \geqslant 0 \ .
\end{aligned}
\right\} \qquad (4.16)
$$

In Eq. (4.16), constraints $g_1(\boldsymbol{x})$ and $g_3(\boldsymbol{x})$ are related to the geometry of the individual fins, while constraints $g_2(\boldsymbol{x})$ and $g_4(\boldsymbol{x})$ are related to the configuration of the fin array. Constraint $g_1(\boldsymbol{x})$ ensures the existence of the individual fins by making the outer radius (r_o) greater than the predefined radius at the base (r_b), while constraint $g_2(\boldsymbol{x})$ restricts the half thickness of the individual fins at the base (t_b) to such a value that an array of fins can be formed by accommodating a minimum of two fins within the limited predefined length (W) of the primary surface. Constraint $g_3(\boldsymbol{x})$ makes t_o (half-thickness at the tip of the individual fins) smaller than t_b ensuring that the fins are tapered in shape with the thickness gradually decreasing in the radially outward direction. On the other hand, constraint $g_4(\boldsymbol{x})$ forms the fin array with the lower limit for two fins and the upper limit avoiding the excess number of fins over the length (W) of the primary surface ($s_{\max}$ and $s_{\min}$ are, respectively, the minimum and maximum fin inter-spacing). Finally, the last line in Eq. (4.16) ensures the non-negativity of r_o, t_b and t_o.

In order to avoid any safety hazard resulting from a weak slender tip, the half

thickness of the fins at the tip (i.e., t_o) may be maintained at some specified minimum value. Also, the outer radius of the fins may be made sufficiently larger than the fin thickness (i.e., $r_o \ggg 2t_b$) so that one-dimensional heat transfer by conduction through each fin can be assumed.

In Eq. (4.16), the maximization of the heat transfer rate (f_1) and the surface efficiency (f_4) would enhance the overall performance of the fin array, while the minimization of the induced maximum thermal stress in a fin (f_2) would increase the life span of the fin array and the minimization of the total volume of the fins (f_3) will lower the production cost by reducing the required amount of fin material. These objective functions, in terms of the notations and formulation of the thermal model of the fin array as presented in Section 4.2, can be formulated as given by Eq. (4.17).

$$f_1(\boldsymbol{x}) = n_{\text{fin}} \times \left\{ -kA_b \left.\frac{dT}{dr}\right|_{r=r_b} + hA_{\text{sp}}(T_b - T_\infty) \right\} \tag{4.17a}$$

$$f_2(\boldsymbol{x}) = \left[\left(\sigma_r^2 - \sigma_r\sigma_\theta + \sigma_\theta^2\right)^{\frac{1}{2}} \right]_{\text{max}} \tag{4.17b}$$

$$f_3(\boldsymbol{x}) = n_{\text{fin}} \times \frac{4}{3}\pi \sum_{n=2,4,\ldots}^{N} r_{n-1}(r_n - r_{n-1})(t_{n-2} + 4\,t_{n-1} + t_n) \tag{4.17c}$$

$$f_4(\boldsymbol{x}) = \frac{1}{n_{\text{fin}}} \times \frac{f_1(\boldsymbol{x})}{hA_s(T_b - T_\infty) + hA_{\text{sp}}(T_b - T_\infty)} \tag{4.17d}$$

where, $\quad A_b = 4\pi r_b t_b \tag{4.17e}$

$$A_{sp} = 2\pi r_b s_b \tag{4.17f}$$

$$A_s = 4\pi r_o t_o + 2\pi \sum_{n=1}^{N} (r_n + r_{n-1})\left\{(r_n - r_{n-1})^2 + (t_{n-1} - t_n)^2\right\}^{\frac{1}{2}} \tag{4.17g}$$

In Eq. (4.17c), the volume (i.e., f_3) of a fin is evaluated using the Simpson's $\frac{1}{3}$ rule for numerical integration. Further, the heat transfer surface area (i.e., A_s) of a fin is evaluated in Eq. (4.17g) from the geometry of the fin.

4.2.4   Solution procedure

The multi-objective formulation of the design of an array of identical annular fins having plane fin profiles with trapezoidal shape, as expressed by Eq. (4.16), is solved by real-coded multi-objective optimizer, the non-dominated sorting genetic algorithm II (NSGA-II).

4.2.4.1   Constraints handling through variable bounds

Though the design of a fin array is formulated in Eq. (4.16) as a constrained optimization problem, it can easily be handled as an unconstrained optimization problem.

Since r_b (radius of a fin at its base) is a predefined fixed parameter, constraint $g_1(\boldsymbol{x})$ can be made satisfied automatically by fixing $(r_b, r_{\max}]$ as the range of r_o (outer radius of the fin), where $r_{\max}$ is the allowable upper limit of r_o.

Similarly, constraint $g_2(\boldsymbol{x})$ can be made satisfied simply by fixing t_b (fin half-thickness at the base) in the range of $\left[t_{\min}, \frac{W}{4}\right]$, where $t_{\min}$ is the allowable lower limit of t_b. It is to be noted that the maximum half-thickness of a fin could be $\frac{W}{4}$, but it may be taken to be $t_{\max} \ll \frac{W}{4}$ such that one-dimensional heat flow through the fin can be considered.

Since both t_o (fin half-thickness at the tip) and t_b are variables, constraint $g_3(\boldsymbol{x})$ can be made satisfied by sorting their distinct values in ascending order, i.e., generating two distinct values for both variables in the range of $[t_{\min}, t_{\max}]$ and then assigning the smaller value to t_o and the other one to t_b.

The satisfaction of constraint $g_4(\boldsymbol{x})$ automatically is a little bit tricky. For this, the range $[s_{\min}, s_{\max}]$ for fin inter-spacing is to be so chosen that the air flowing through two consecutive fins would maintain the Rayleigh number in the laminar range of $[5, 10^8]$. Accordingly, the range $[s_{\min}, s_{\max}]$ may be obtained through a reserve calculation. Since the Rayleigh number (Ra) as expressed in Eq. (4.1) is

a function only of the fin mean inter-spacing (s_m) and the fin outer radius (r_o) keeping all other terms constant for a given scenario, s_m can be computed as $s_{\min}$ by replacing r_o by $r_{\max}$ and Ra by its lower limit of 5. Similarly, s_m can be computed as $s'_{\max}$ by replacing r_o by $r_{\min}$ and Ra by its upper limit of 10^8, where $s'_{\max}$ is the maximum fin inter-spacing at the tip and $r_{\min}$ ($r_{\min} > r_b$) is the allowable minimum value of r_o. The value of $s_{\max}$ is finally obtained by deducting $2(t_{\max} - t_{\min})$ from $s'_{\max}$.

Once all the four constraints are made satisfied automatically as above, the equal fin inter-spacing (s_b) for all the adjacent pairs of fins can be obtained using Eq. (4.18).

$$s_b = \frac{W}{n_{\text{fin}}} - 2t_b \ . \tag{4.18}$$

4.2.4.2 Evaluation of objective values

In every loop (iteration) of an optimizer, the values of the four objective functions given by Eqs. (4.17a)–(4.17d) will be required, which are to be evaluated numerically. The heat transfer rate, f_1 given by Eq. (4.17a) is to be evaluated by solving the problem governing Eq. (4.14) along with its associated boundary conditions expressed by Eq. (4.15). Similarly, the induced maximum thermal stress, f_2 given by Eq. (4.17b) is to be evaluated by solving the problem governing Eq. (3.19) along with its associated boundary conditions expressed by Eq. (3.20). For these purpose, the hybrid spline difference method (HSDM) can be employed for evaluating the dimensionless temperature field (ω) by solving Eqs. (4.14) and (4.15), and the displacement field (ψ) by solving Eqs. (3.19) and (3.20). The results of HSDM for annular fin with continuously varying thickness are already validated with published results of another numerical method in Section 3.2.4.

In HSDM, the region of study can be discretized as given by Eq. (A.9).

The following is the detail procedure for evaluating f_1 and f_2 through the HSDM scheme expressed by Eq. (A.9):

(a) Discretize Eqs. (4.14) and (4.15) using Eq. (A.9).

(b) Evaluate p_n $(n = 0, 1, \ldots, N)$ by solving the discretized forms of Eqs. (4.14) and (4.15), which can be done through the variant of the Thomas algorithm proposed by Martin and Boyd [64].

(c) At all the grid points, evaluate the dimensionless temperature distribution and their derivatives up to the second order, i.e., ω_n, ω_n' and ω_n'', using the values of p_n in Eq. (A.9).

(d) Evaluate the temperature gradient at the base of the fin, i.e., $\frac{dT}{dr}\big|_{r=r_b}$, using the dimensionless temperature gradient ω_o' at the base of the fin.

(e) Evaluate f_1 using the value of $\frac{dT}{dr}\big|_{r=r_b}$ in Eq. (4.17a).

(f) Repeat Steps (a) and (b) for Eqs. (3.19) and (3.20), and then evaluate the dimensionless displacement and their derivatives up to the second order (i.e., ψ_n, ψ_n' and ψ_n'') using the obtained values of p_n in Eq. (A.9).

(g) Throughout the fin length in the radial direction, evaluate the displacement field (u), along with their first order gradient $(\frac{du}{dr})$ using the values of ψ_n and ψ_n'.

(h) Evaluate the radial and circumferential thermal stresses (i.e., σ_r and σ_θ, respectively) throughout the fin length using the temperature distribution, and the displacement field and its first order derivative in Eq. (3.14).

(i) Calculating the resultants of σ_θ and σ_r throughout the fin length, take their maximum value as f_2.

4.2.5   Numerical experimentation and discussion

The present study revolves around the analysis of an array of identical annular trapezoidal fins, considering a constant temperature at the base of the fins, heat dissipation from the fin surfaces to the surroundings by natural convection only, and variable thermal conductivity of the fin material.

The operating conditions, thermal properties of the fin material and the fin array configuration with reference to Fig. 4.7(a), considered for numerical experimentation, are given in Table 4.2. Further, selecting NSGA-II (Deb et al. [23]) as the

Table 4.2: Operating conditions, fin material properties, and fin array configuration for linearly varying thickness fin array.

Parameter	Value/ range of value
Ambient temperature (T_∞)	300 K
Temperature at the base of the fins (T_b)	373 K
Thermal conductivity of the fin material at T_∞ (k_a)	186 W/mK
Parameter for variable thermal conductivity (β)	-0.00018 K^{-1}
Base radius of the fin (r_b)	2.0 cm
Length of the primary cylinder (W)	40.0 cm
Fin inter-spacing $(s_{\min}, s_{\max})$	[0.45, 18.0] cm
Outer radius of the fins $((r_{\min}, r_{\max})$ for $r_o)$	[2.5, 15.0] cm
Fin half thickness at the base and tip $((t_{\min}, t_{\max})$ for t_b and $t_o)$	[0.01, 0.2] cm

optimizer, its algorithmic parameter values are given in Table 3.3. With such input values, the optimization of the fin array configuration, as formulated in Eq. (4.16), is analyzed under two scenarios. In the first scenario, all the objective functions, $f_1(\boldsymbol{x})$–$f_4(\boldsymbol{x})$ given by Eq. (4.16), are optimized in various pairs, while all the four objective functions are optimized simultaneously in the second scenario.

4.2.5.1 Scenario I

The primary aim of the present study is to optimize the fin array configuration by simultaneously maximizing the total heat transfer rate (f_1) from the fin array and minimizing the thermal stress (f_2) induced in an individual fin of the array. Further, the fin array configuration at hand is optimized for maximizing the total heat transfer rate (f_1) of the fin array separately with minimizing the fin volume (f_3) of the fin array and maximizing the surface efficiency (f_4) of the fin array. The final Pareto fronts obtained in the respective cases are shown in Figs. 4.8(a)–4.8(c), respectively. In Fig. 4.8(a), the solutions of the Pareto front depict the conflicting nature between the total heat transfer rate and the thermal stress induced in an individual fin of the fin array. Similar conflicting nature of the total fin volume and the surface efficiency of the fin array with the total heat transfer rate from the fin array can be seen in Figs. 4.8(b) and 4.8(c), respectively.
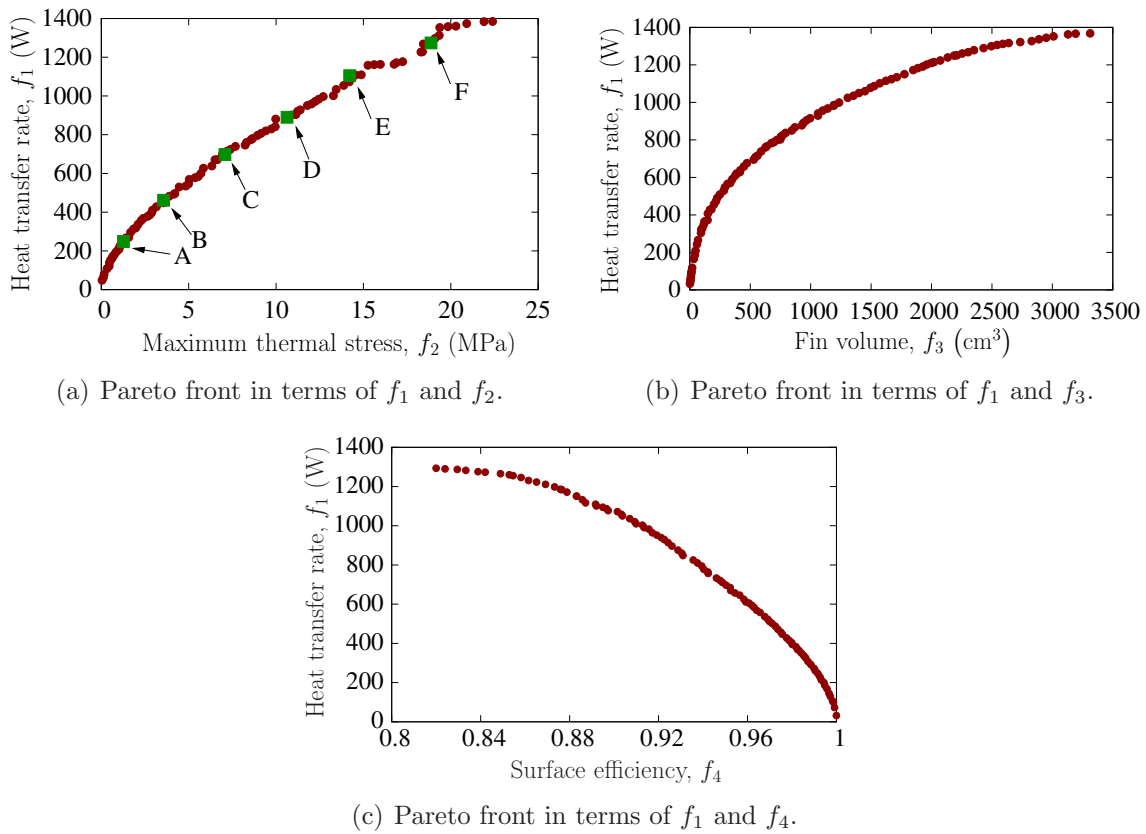
(a) Pareto front in terms of f_1 and f_2.

(b) Pareto front in terms of f_1 and f_3.

(c) Pareto front in terms of f_1 and f_4.

Figure 4.8: Pareto fronts for pairwise objective functions.

Corresponding to trade-off solutions A–F of Fig. 4.8(a), six selective efficient fin array configurations are shown in Fig. 4.9, where the variations in the patterns of the individual fin profiles as well as in the number of fins in the fin array are noticeable (since the length of the primary cylindrical surface is fixed, a variation in the number of fins in the fin array implies a variation in the fin inter-spacing also). The values of the other two objective functions, f_3 and f_4, for these fin array configurations are also calculated and shown in Fig. 4.9 alongside the optimized values of f_1 and f_2. It is observed in these particular six fin array configurations that, f_3 also increases continuously with increasing f_1 and f_2, but f_4 decreases.

4.2.5.2   Scenario II

It is found in Section 4.2.5.1 that when the objective functions are optimized in various pairs, the heat transfer rate varies differently with different objective functions, without following any certain pattern. Hence, in order to arrive at a general conclu-
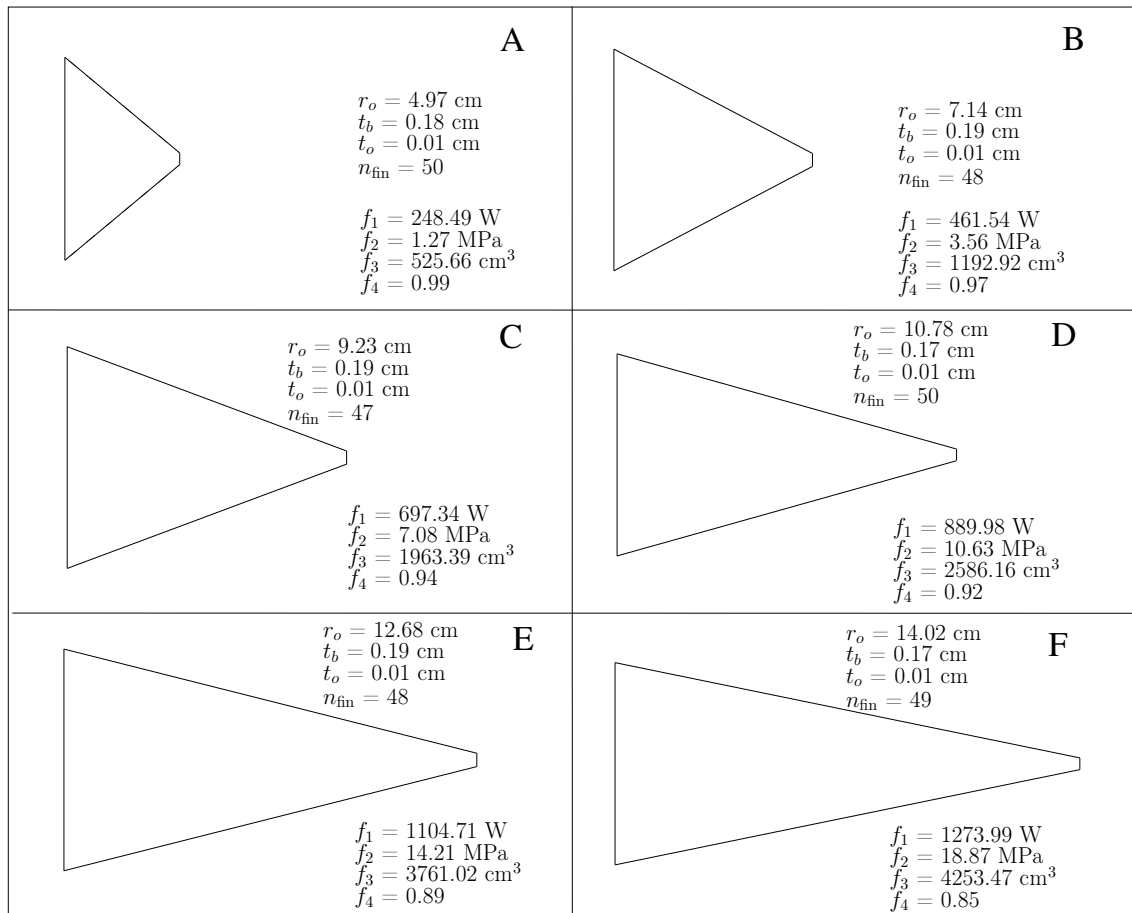
Figure 4.9: Selective efficient fin geometries (corresponding to trade-off solutions A–F of Fig. 4.8(a). In these plots, the scale along the axial (vertical) direction is 15 times larger than that along the radial (horizontal) direction.)

sion, all the four objective functions, i.e., f_1–f_4 given in Eq. (4.16), are optimized here simultaneously.

The four-dimensional Pareto front obtained in the present case is plotted in a parallel coordinate system as shown in Fig. 4.10, where the conflicting nature of various objective functions is clearly visible. For instance, the solution of the Pareto front having the lowest thermal stress value (i.e., the f_2 value) exhibits the lowest fin volume (i.e., the f_3 value) and heat transfer rate (i.e., the f_1 value) and a very high surface efficiency (i.e., the f_4 value).

The simultaneous optimization of all the considered four objective functions is well justified by the fact that a practical scenario would always desire to optimize the possible maximum number of objective functions. Further, from the Pareto front
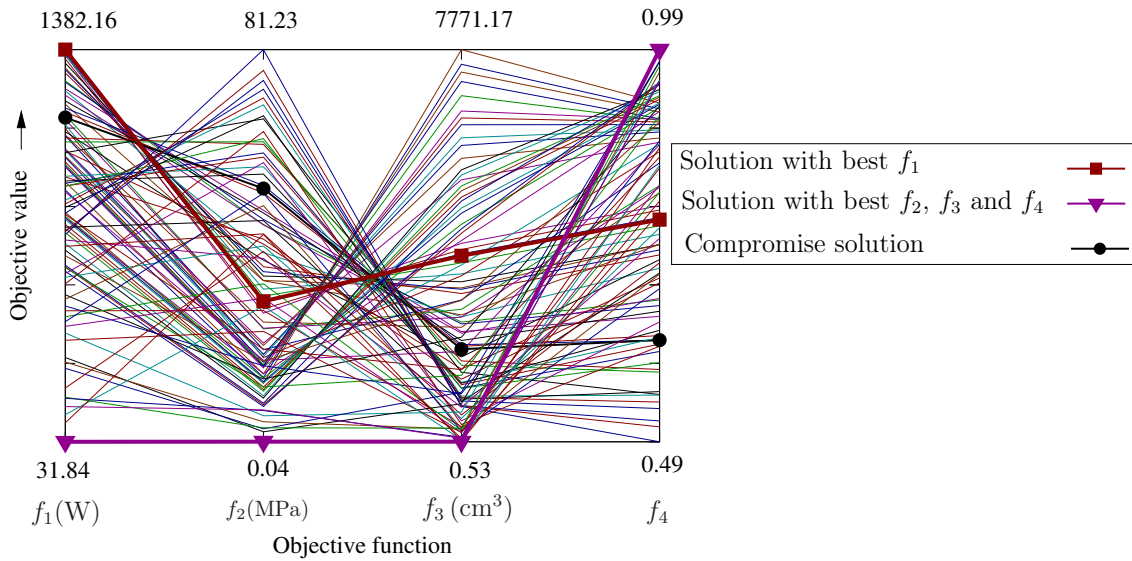
**Figure 4.10:** Four-dimensional Pareto front in two-dimensional parallel coordinate system.

obtained by optimizing a number of objective functions simultaneously, as shown in Fig. 4.10, a designer can clearly understand the relationships among different objective functions. Thus, the designer can enjoy the flexibility of adopting a compromise solution from the Pareto front, based upon his or her accessibility and practicability of the available information and resources for the problem at hand. One such compromise solution, bearing some balanced values of the considered four objective functions, is also shown in Fig. 4.10.

4.2.6   Sensitivity analysis

Finally, a sensitivity analysis is performed in order to investigate the responses of the total heat transfer rate from the fin array and the maximum thermal stress developed in an individual to any change in the design variables of the studied fin array.

For this purpose, an arbitrary fin array configuration of $(t_b^\dagger, t_o^\dagger, r_o^\dagger, n_{\text{fin}}^\dagger) = (0.06 \text{ cm},$ $0.016 \text{ cm}, 9.25 \text{ cm}, 20)$ is considered, corresponding to which the heat transfer rate $(f_1^\dagger)$ from the fin array and the developed maximum thermal stress $(f_2\dagger)$ in an individual fin will be 342.14 W and 25.53 MPa, respectively. To carry out the

sensitivity analysis, the problem at hand is solved four times, each time allowing a distinct design variable to vary by 40% in either directions from its value in the considered fin configuration, while keeping the other three design variables fixed. The plots of the corresponding variations in the total heat transfer rate from the fin array and the maximum thermal stress developed in an individual fin are shown in Figs. 4.11(a) and 4.11(b), respectively.
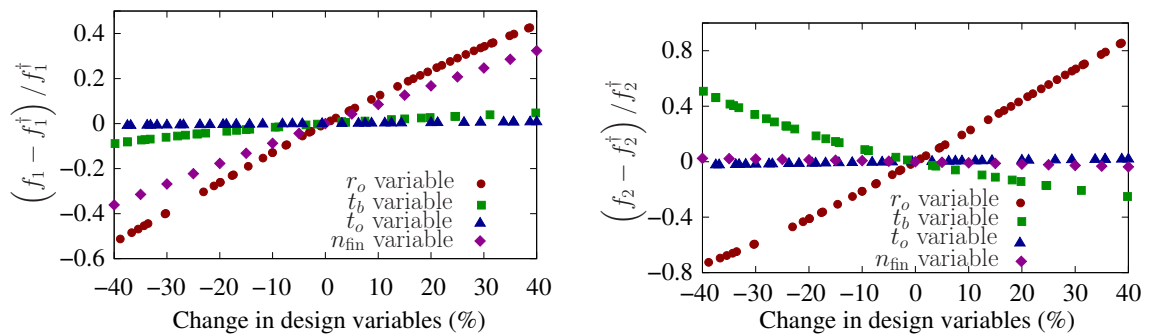
(a) Variation of the heat transfer rate with the design variables.

(b) Variation of the maximum thermal stress with the design variables.

Figure 4.11: Sensitivity analysis of heat transfer rate and maximum thermal stress in terms of design variables.

It is observed in the plots of Fig. 4.11 that both heat transfer rate and thermal stress are highly sensitive to the outer radius (r_o) of the fins. In the case of the heat transfer rate, the next highly sensitive design variable is the number of fins (n_{fin}), followed by the fin cross-sectional half thickness at the base (t_b). On the other hand, for the developed maximum thermal stress, the fin cross-sectional half thickness at the base (t_b) is more sensitive than the number of fins (n_{fin}). The influence of the fin cross-sectional half thickness at the outer radius (t_o) is comparatively very less in both cases. Accordingly, in order to acquire the desired heat transfer effect maintaining the maximum thermal stress to a minimum, a designer will have the freedom to choose economic combinations of the design variables based upon the accessibility and practicability of the available information and resources.

It may also be noticed in Fig. 4.11 that with an increase in t_b, the heat transfer rate in the fin array increases, while the induced maximum thermal stress decreases. Since problem related all other parameter values were kept constant, this happened because of the fact that an increase in t_b decreases the conductive resistance to

heat flow, thus the heat transfer rate increases. Further increased heat transfer rate results in a more uniform temperature distribution along the radial direction of a fin, which leads to a decrease in the thermal stress in the fin.

4.3 Fin array of non-linearly varying thickness fins

In the present study, an annular fin array with individual fins of non-linearly varying thickness defined by a B-spline curve is investigated here with the assumptions that Poisson's ratio, coefficient of thermal expansion, and modulus of elasticity of the fin material remain constant irrespective of any variation in temperature and the inner and outer radii of the fin are free of traction

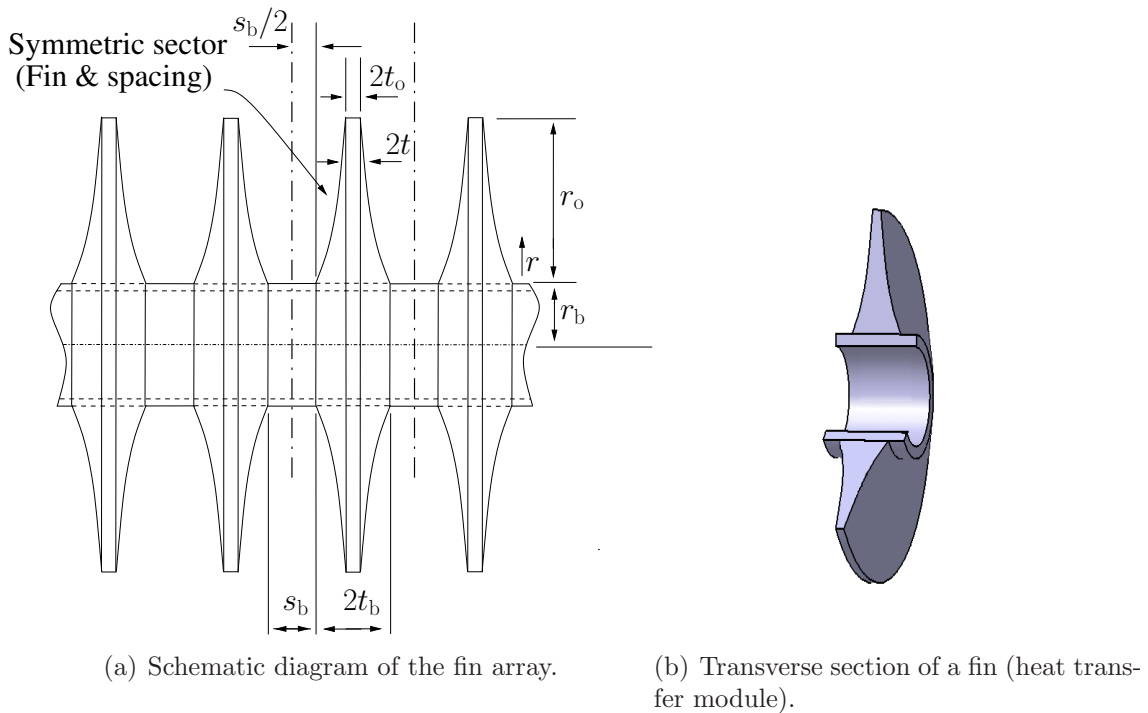Fig. 4.12(a) shows the schematic diagram of an annular fin array with individual

(a) Schematic diagram of the fin array.

(b) Transverse section of a fin (heat transfer module).

Figure 4.12: Array of identical annular fins with nonlinear varying profile (and equal fin inter-spacing.)

fins having nonlinear profiles. In Fig. 4.12(a), n_{fin} is the number of fins in the fin

array, r represents the radius of a fin with r_o and r_b as its values respectively at the tip and base of the fin, t represents the half-thickness of a fin with t_o and t_b as its values respectively at the tip and base of the fin, s_b is the spacing between the bases of two adjacent fins (fin inter-spacing), and W is the total length of the primary surface.

The fin array shown in Fig. 4.12(a) is actually a repetitive surface containing one fin and spacing as shown separately in Fig. 4.12(b). Hence, the thermal analysis for the entire fin array will be equivalent to that for such a single repetitive symmetric sector (heat transfer module).

4.3.1 Formulation for heat transfer equation

The formulation for heat transfer equation of non-linearly varying thickness annular fin array is similar to that of linearly varying thickness annular fin array as given in Section 4.2.1.

4.3.2 Formulation of the thermal stress model

The formulation of the thermal stress model of non-linearly varying thickness annular fin array is similar to that of linearly varying thickness annular fin array as given in Section 4.2.2.

4.3.3 Optimization modeling

In the present study the performance of the considered fin array is evaluated in terms five objective functions in different combinations, which are the heat transfer rate from the fin array, maximum thermal stress induced in an individual fin, total fin volume of the array, surface efficiency, and argumentation factor of the fin array. The fin array configuration is defined in terms of the control points of the B-spline

curve forming the profile of a fin and the total numbers of fins in the fin array. Hence, any change in the value of any of these control points and the total number of fins in the fin array will change the fin array configuration with some new values of the five performance functions.

Hence, the design of the considered annular fin array is modeled as a multi-objective optimization problem with the five performance functions as the objective functions, while the control points of the B-spline curve and the total number of fins in the array as the design variables. The control points are so taken that the extreme two will be at the two ends (base and tip) of the fin and the intermediate ones are distributed along the radial direction of the fin, while they in the axial direction will give the half-thickness of the fin at different points. In other words, say, the x-coordinates of the control points are distributed along the radial direction of the fin and their y-coordinates are the half-thickness of the fin. Further, in order to have a practical nonlinear fin profile, the y-coordinate values are gradually decreased with their increasing x-coordinate values, i.e., in the radially outward direction of the fin. Accordingly, the optimization model of the annular fin array design problem can be formulated as expressed by Eq. (4.19).

$$
\left.
\begin{aligned}
\text{Determine} \quad & \boldsymbol{x} \;\equiv\; (n_{\text{fin}}, P_1, P_2, P_3, \cdots\cdots, P_m)^{\mathrm{T}} \\
\text{to maximize} \quad & \boldsymbol{z}(\boldsymbol{x}) \;\equiv\; \{f_1(\boldsymbol{x}), f_4(\boldsymbol{x}), f_5(\boldsymbol{x})\} \\
\text{minimize} \quad & \boldsymbol{f}(\boldsymbol{x}) \;\equiv\; \{f_2(\boldsymbol{x}), f_3(\boldsymbol{x})\} \\
\text{subject to} \quad & g_1(\boldsymbol{x}) \;\equiv\; x_1 < x_2 \leqslant \cdots \leqslant x_m \\
& g_2(\boldsymbol{x}) \;\equiv\; \tfrac{W}{4} \geqslant y_1 \geqslant y_2 \geqslant \cdots \geqslant y_m \\
& g_3(\boldsymbol{x}) \;\equiv\; \left\lceil \tfrac{W}{2y_1+s_{\max}} \right\rceil \leqslant n_{\text{fin}} \leqslant \left\lfloor \tfrac{W}{2y_1+s_{\min}} \right\rfloor \\
& s_{\max}, s_{\min} \geqslant 0 \; .
\end{aligned}
\right\}
\tag{4.19}
$$

In Eq. (4.19), $P_i = (x_i, y_i)$ is the ith control point and m is the total number of control points of the B-spline curve defining the profile of individual fins of the fin array. Constraint $g_1(\boldsymbol{x})$ makes the control points of the B-spline curve (i.e., their x-coordinate values) distributed along the radially downward direction of a fin and constraint $g_2(\boldsymbol{x})$ ensures that their corresponding y-coordinate values are

non-increasing, where $x_1 = r_b$, $y_1 = t_b$, $x_m = r_o$ and $y_m = t_o$ as considered in the schematic diagram of the fin array configuration shown in Fig. 4.12(a). In constraint $g_2(\boldsymbol{x})$, the upper limit of y_1 (i.e., $y_1 \leqslant \frac{W}{4}$) restricts the half thickness of the individual fins at the base (t_b) to such a value that fin array can be formed by accommodating a minimum of two fins within the limited predefined length (W) of the primary surface (in practice, $y_1 \ll \frac{W}{4}$ if the heat transfer from the fins is to be studied as one-dimensional). Since a sharp thickness at the edge of a fin may pose safety hazard, the value of y_m may also be restricted to a finite value within a reasonable range as widely practiced in real-life applications. Finally, constraint $g_3(\boldsymbol{x})$ ensures the existence of an fin array by setting the lower limit of the number of fins to be two and the upper limit to such a value to avoid the excess number of fins over the length (W) of the primary surface. The range of fin inter-spacing at the base, $(s_{\min}, s_{\max})$, is to be chosen in constraint $g_3(\boldsymbol{x})$ in such a way that Ra remains within the laminar range (see Eq. (4.1)).

In Eq. (4.19), $f_1(\boldsymbol{x})$–$f_5(\boldsymbol{x})$ are the five objective functions, which represent respectively the heat transfer rate from the fin array, maximum thermal stress developed in an individual fin of the array, total fin volume of the array, surface efficiency of the fin array, and augmentation factor of the fin array. The overall thermal performance of the fin array will be enhanced on maximizing $f_1(\boldsymbol{x})$, $f_4(\boldsymbol{x})$ and $f_5(\boldsymbol{x})$, while its life expectancy would be enhanced by minimizing $f_2(\boldsymbol{x})$ and the cost of the fin material will be reduced by minimizing $f_3(\boldsymbol{x})$. These objective functions, in terms of the notations and formulations of heat transfer equation of the fin array and the thermal stress model as presented in the Sections 4.3.1 and 4.3.2 respectively, can be expressed by Eq. (4.20).

$$f_1(\boldsymbol{x}) = n_{\text{fin}} \times \left\{ -kA_b \left. \frac{dT}{dr} \right|_{r=r_{\text{b}}} + hA_{\text{sp}} \left(T_b - T_\infty \right) \right\} \tag{4.20a}$$

$$f_2(\boldsymbol{x}) = \left\{ \left(\sigma_r^2 - \sigma_r \sigma_\theta + \sigma_\theta^2 \right)^{\frac{1}{2}} \right\}_{\max} \tag{4.20b}$$

$$f_3(\boldsymbol{x}) = n_{\text{fin}} \times \frac{4\pi}{3} \sum_{n=2,\ 4,\ ...}^{N} r_{n-1} \left(r_n - r_{n-1} \right) \left(t_{n-2} + 4\ t_{n-1} + t_n \right) \tag{4.20c}$$

$$f_4(\boldsymbol{x}) = \frac{1}{n_{\text{fin}}} \times \frac{f_1(\boldsymbol{x})}{\left\{ hA_s \left(T_b - T_\infty \right) + hA_{\text{sp}} \left(T_b - T_\infty \right) \right\}} \tag{4.20d}$$

$$f_5(\boldsymbol{x}) = \frac{1}{n_{\text{fin}}} \times \frac{f_1(\boldsymbol{x})}{\{hA_b\,(T_b - T_\infty) + hA_{\text{sp}}\,(T_b - T_\infty)\}} \tag{4.20e}$$

$$\text{where,} \qquad A_b = 4\pi r_b t_b \tag{4.20f}$$

$$A_{sp} = 2\pi r_b s_b \tag{4.20g}$$

$$A_s = 4\pi r_o t_o + 2\pi \sum_{n=1}^{N} (r_n + r_{n-1}) \left\{ (r_n - r_{n-1})^2 + (t_{n-1} - t_n)^2 \right\}^{\frac{1}{2}} \tag{4.20h}$$

In Eq. (4.20c), the volume (i.e., f_3) of a fin is evaluated using the Simpson's $\frac{1}{3}$ rule for numerical integration. Further, the heat transfer surface area (i.e., A_s) of a fin is evaluated in Eq. (4.20h) from the geometry of the fin.

4.3.4   Solution procedure

The fin array design formulated in Eq. (4.19) as a multi objective optimization problem is optimized using the non-dominated sorting genetic algorithm II (NSGA-II).

4.3.4.1   Constraints Handling Through Variable Bounds

The design of the fin array is formulated in Eq. (4.19) as a constrained optimization problem. However, it can easily be handled as an unconstrained optimization problem.

Since $x_1\ (= r_b$, the radius of a fin at the base) is predefined, constraint $g_1(\boldsymbol{x})$ can be made satisfied by generating $(m-1)$ number of data in the range of $(r_b, r_{\max}]$ and then sorting them in ascending order as the x-coordinate values (i.e., $x_2, x_3, \cdots, x_m$) of the remaining $(m-1)$ number of control points of the B-spline curve defining the profile of the fin, where $r_{\max}$ is the allowable maximum value of x_m (outer radius of the fin). Similarly, constraint $g_2(\boldsymbol{x})$ can be made satisfied by generating m number of data in the range of $(t_{\min}, t_{\max})$ and then sorting them in descending order as the

corresponding y-coordinate values (i.e., $y_1, y_2, \cdots, y_m$) of the m number of control points of the B-spline curve, where $(t_{\min}, t_{\max})$ is the allowable range of the fin half-thickness $(t_{\max} \leqslant \frac{W}{4})$.

On the other hand, constraint $g_3(\boldsymbol{x})$ can be made satisfied automatically through a reserve computation. Here, the range $(s_{\min}, s_{\max})$ for fin inter-spacing at the base is to be so chosen such that the flow of air through two consecutive fins maintains the Rayleigh number in the laminar range of $[5, 10^8]$. Since for a given scenario, the Rayleigh number (Ra) as expressed in Eq. (4.1) is a function of the fin mean inter-spacing (s_m) and the fin outer radius (r_o) only, s_m can be computed as $s_{\min}$ by replacing r_o by $r_{\max}$ and Ra by its lower limit of 5. Similarly, s_m can be computed as $s'_{\max}$ by replacing r_o by $r_{\min}$ and Ra by its upper limit of 10^8, where $s'_{\max}$ is the maximum fin inter-spacing at the tip and $r_{\min}$ $(r_{\min} > r_b)$ is the allowable minimum value of r_o. Finally, $s_{\max}$ can be obtained by deducting $2(t_{\max} - t_{\min})$ from $s'_{\max}$.

Once all the three constraints are satisfied automatically as above, for all the adjacent pairs of fins, the equal fin inter-spacing at the base (s_b) can be computed using Eq. (4.21).

$$s_b = \frac{W}{n_{\text{fin}}} - 2y_1 \ . \tag{4.21}$$

4.3.4.2 Evaluation of Objective Functions

The evaluation of the objective functions for non-linearly varying thickness annular fin array is similar to that of linearly varying thickness annular fin array as given in Section 4.2.4.2.

4.3.5 Numerical experimentation and discussion

A cubic curve with open uniform knot vector and of order 4 is considered for the B-spline curve representing the fin profile of an individual fin of the fin array system investigated in this work. Further, five control points are considered here to

approximate the fin profile. The coordinates of the five control points along with the number of fins in the studied fin array are considered as the design variables. Further, a constant temperature at the base of the fins along with temperature dependent variable thermal conductivity are considered. Also, heat is transferred to the surrounding from the fin array surface by natural convection only.

With reference to Fig. 4.12(a), Table 4.3 lists the considered operating condi-

Table 4.3: Operating conditions, fin material properties, and fin array geometry for non-linearly thickness fin array.

Parameter	Value/ range of value
Ambient temperature (T_∞)	300 K
Temperature of the fin at the base (T_b)	373 K
Thermal conductivity of the fin material at T_∞ (k_a)	186 W/mK
Parameter for variable thermal conductivity (β)	-0.00018 K^{-1}
Base radius (r_b)	2.0 cm
Length of the primary cylinder (W)	40.0 cm
Fin inter-spacing at base ($s_{\min}, s_{\max}$)	[0.45, 18.0] cm
Outer radius of the fins (($r_{\min}, r_{\max}$) for r_o)	[2.5–15.0] cm
Half thickness of the fin (($t_{\min}, t_{\max}$) for t)	[0.01–0.2] cm

tions and thermal properties of the fin material along with fin array configuration geometry. The user-defined algorithmic parameter settings for NSGA-II are given in Table 3.3. With the sets of input parameters as above, the fin array optimization problem formulated in Eq. (4.19) is investigated under two scenarios. In the first scenario, the objective function f_1–f_5 given by Eq. (4.20) are optimized in various pairs, while all the five objective functions are optimized simultaneously in the second scenario.

4.3.5.1   Scenario I

At the first instance, the fin array configuration is optimized considering maximization of the heat transfer rate (f_1) and minimization of the maximum thermal stress (f_2) developed in individual fins. The obtained Pareto front, shown in Fig. 4.13(a), contains a set of trade-off solutions in terms of f_1 and f_2. The conflicting nature of the two chosen objective functions is clearly depicted in the figure. Six number of selective efficient fin array configurations, corresponding to trade-off
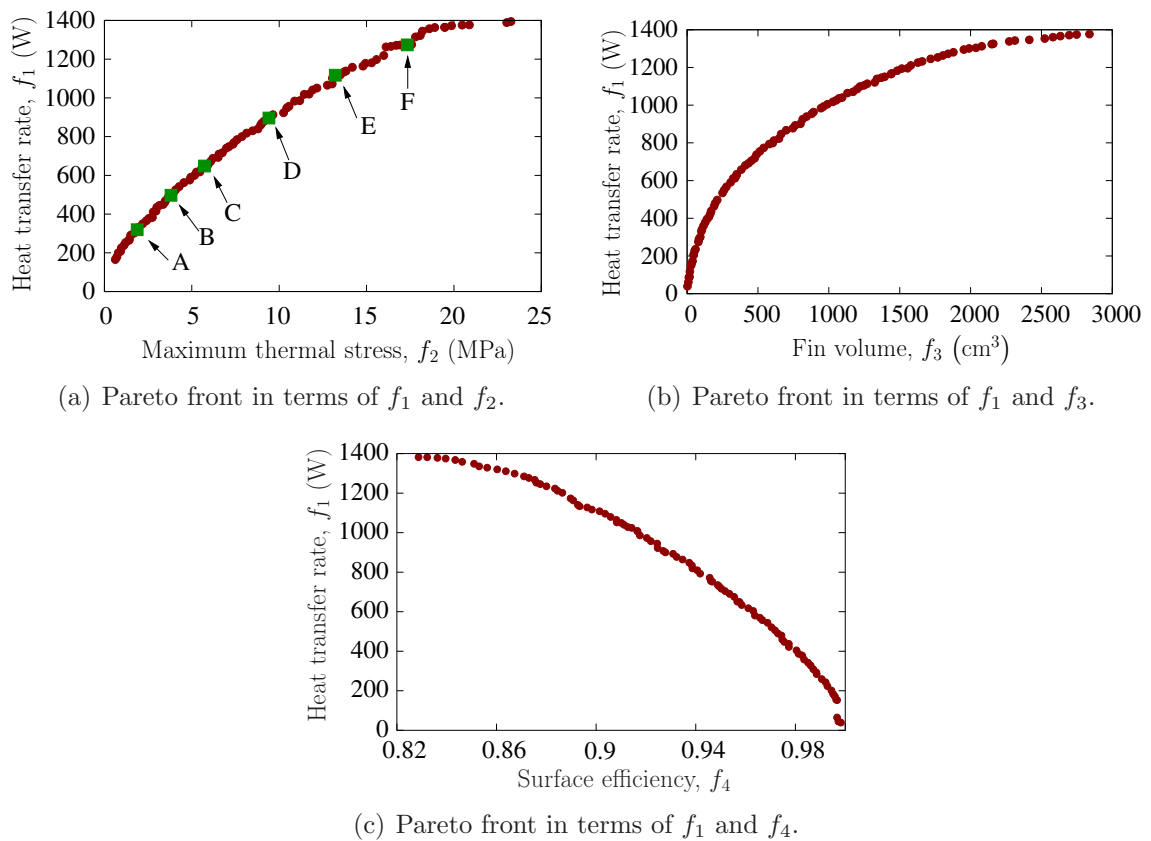
(a) Pareto front in terms of f_1 and f_2.

(b) Pareto front in terms of f_1 and f_3.

(c) Pareto front in terms of f_1 and f_4.

Figure 4.13: Pareto fronts for pairwise objective functions..

solutions A–F of Fig. 4.13(a), are shown in Fig. 4.14, where the patterns of variation of the individual fin profiles are noticeable. The values of other three objective functions, f_3–f_5, for these fin configurations are also evaluated and shown in Fig. 4.14. It is observed that f_3 and f_5 continue to increase with increasing f_1 and f_2, while f_4 shows the reverse trend.

In view of above, the fin array configuration is studied in the second step for maximization of f_1 separately with minimization of f_3 and maximization of f_4. The obtained final Pareto fronts for these two cases are shown respectively in Figs. 4.13(b) and 4.13(c), where also f_1 is found conflicting with both f_3 and f_4. Next, for the points in Fig 4.13(c), the surface efficiency and augmentation factor are plotted in Fig 4.15, where these two objective functions are also found conflicting.
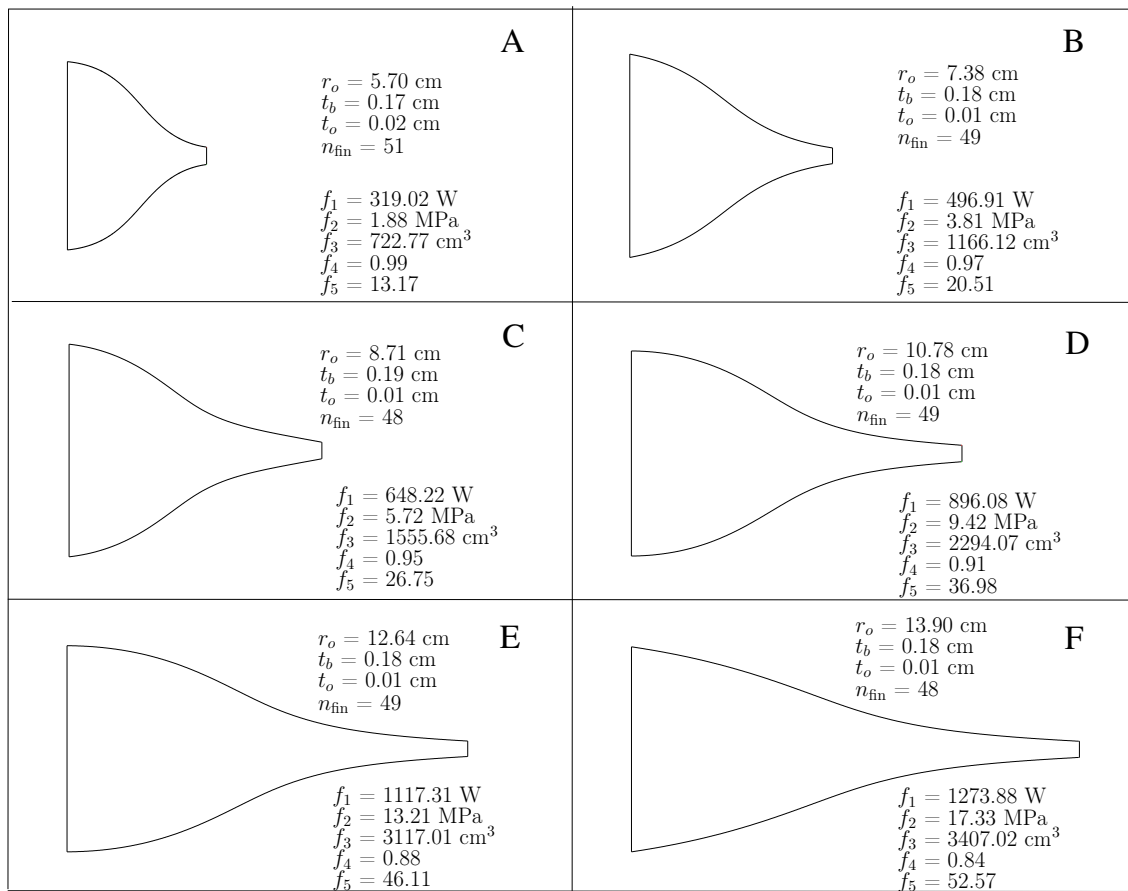
A

$r_o = 5.70$ cm
$t_b = 0.17$ cm
$t_o = 0.02$ cm
$n_\mathrm{fin} = 51$

$f_1 = 319.02$ W
$f_2 = 1.88$ MPa
$f_3 = 722.77$ cm^3
$f_4 = 0.99$
$f_5 = 13.17$

B

$r_o = 7.38$ cm
$t_b = 0.18$ cm
$t_o = 0.01$ cm
$n_\mathrm{fin} = 49$

$f_1 = 496.91$ W
$f_2 = 3.81$ MPa
$f_3 = 1166.12$ cm^3
$f_4 = 0.97$
$f_5 = 20.51$

C

$r_o = 8.71$ cm
$t_b = 0.19$ cm
$t_o = 0.01$ cm
$n_\mathrm{fin} = 48$

$f_1 = 648.22$ W
$f_2 = 5.72$ MPa
$f_3 = 1555.68$ cm^3
$f_4 = 0.95$
$f_5 = 26.75$

D

$r_o = 10.78$ cm
$t_b = 0.18$ cm
$t_o = 0.01$ cm
$n_\mathrm{fin} = 49$

$f_1 = 896.08$ W
$f_2 = 9.42$ MPa
$f_3 = 2294.07$ cm^3
$f_4 = 0.91$
$f_5 = 36.98$

E

$r_o = 12.64$ cm
$t_b = 0.18$ cm
$t_o = 0.01$ cm
$n_\mathrm{fin} = 49$

$f_1 = 1117.31$ W
$f_2 = 13.21$ MPa
$f_3 = 3117.01$ cm^3
$f_4 = 0.88$
$f_5 = 46.11$

F

$r_o = 13.90$ cm
$t_b = 0.18$ cm
$t_o = 0.01$ cm
$n_\mathrm{fin} = 48$

$f_1 = 1273.88$ W
$f_2 = 17.33$ MPa
$f_3 = 3407.02$ cm^3
$f_4 = 0.84$
$f_5 = 52.57$

Figure 4.14: Selective fin array geometries (corresponding to trade-off solutions A–F of Fig. 4.13(a). In these plots, the scale along the axial (vertical) direction is fifteen times larger than that along the radial (horizontal) direction.)
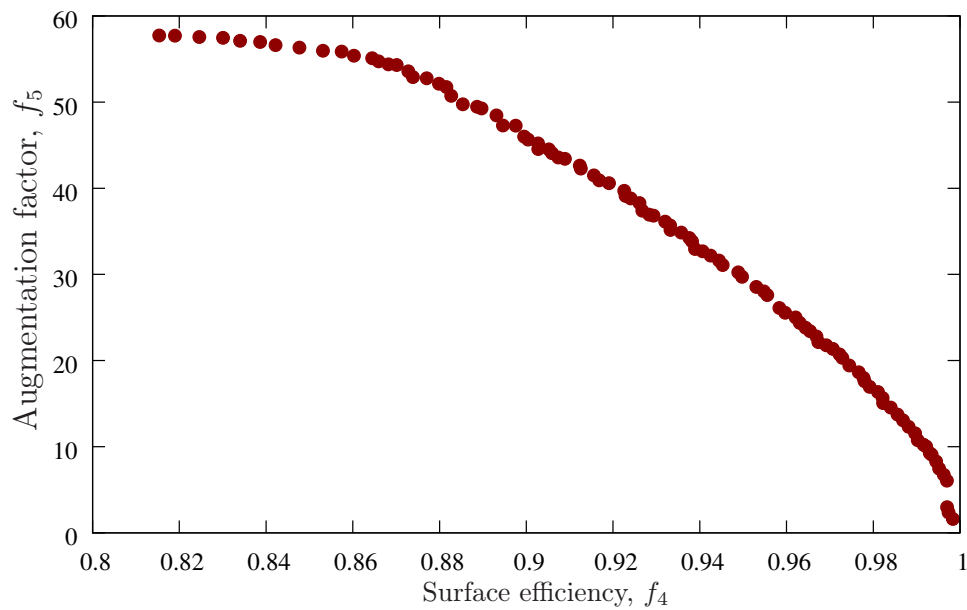
Figure 4.15: Surface efficiency versus augmentation factor (for points of Pareto front in Fig 4.13(c).

4.3.5.2 Scenario II

Optimizing the objective functions in pairs, it is observed in Section 4.3.5.1 above that the variation of the heat transfer rate with other objective functions does not follow any common pattern. In such a situation, in order to arrive at a general scenario, all the five objective functions, i.e., f_1–f_5 given by Eq. (4.20), are optimized here simultaneously. Since it is difficult to analyze a five-dimensional plot on a two-dimensional page, the parallel coordinate system [88] is used to visualize the objective functions as shown in Fig. 4.16.
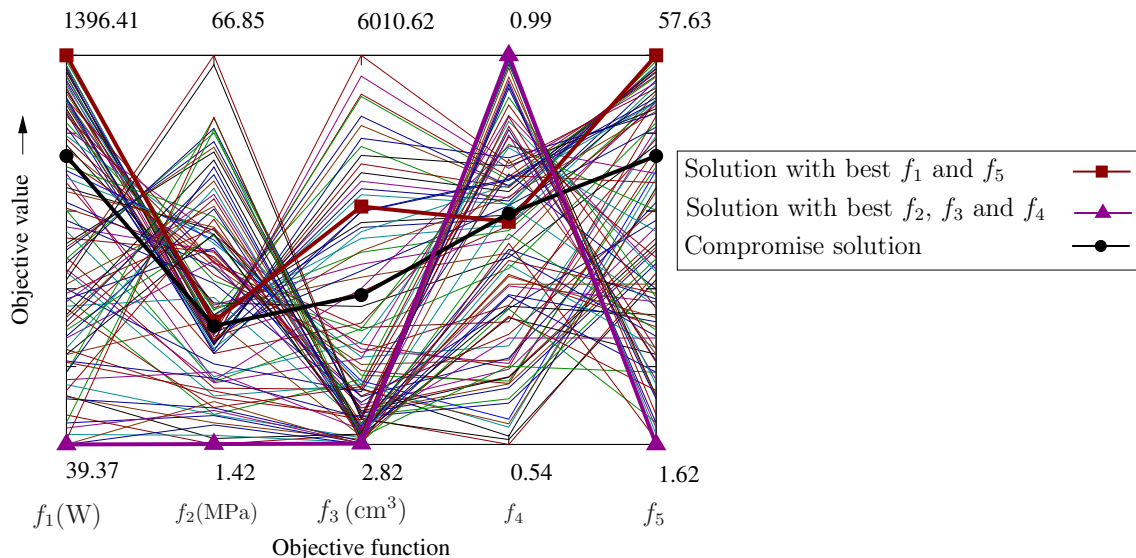
Figure 4.16: Five-dimensional Pareto in the parallel coordinate system.

The overall nature of an objective function with reference to other objective functions can be observed from the plots in the parallel coordinate system as shown in Fig. 4.16. For example, the solution corresponding to the developed minimum thermal stress bears a very low heat transfer rate, fin volume and augmentation factor, while a very high surface efficiency. Hence, it is up to a designer to adopt a balanced solution, out of multiple trade-off solutions of a Pareto front, based upon the availability of information and resources for the problem at hand. Such a compromise solution, having some intermediate objective values, is shown in Fig. 4.16 by a thick crossed line.

4.4   Comparison of different fin arrays

The comparative analysis of annular fin arrays of various profiles (namely step change in thickness, non-linearly varying thickness, and uniform thickness) attached to heat exchangers of cylindrical primary surfaces is the problem taken up in the present study. The schematic diagrams of annular fin arrays with fins having uniform thickness is shown in Fig. 4.17 whereas fin array with fins of step change in thickness and non-linearly varying thickness are already shown as in Figs. 4.1(a) and 4.12(a) respectively. Here, the radial distance is represented by r with its values at
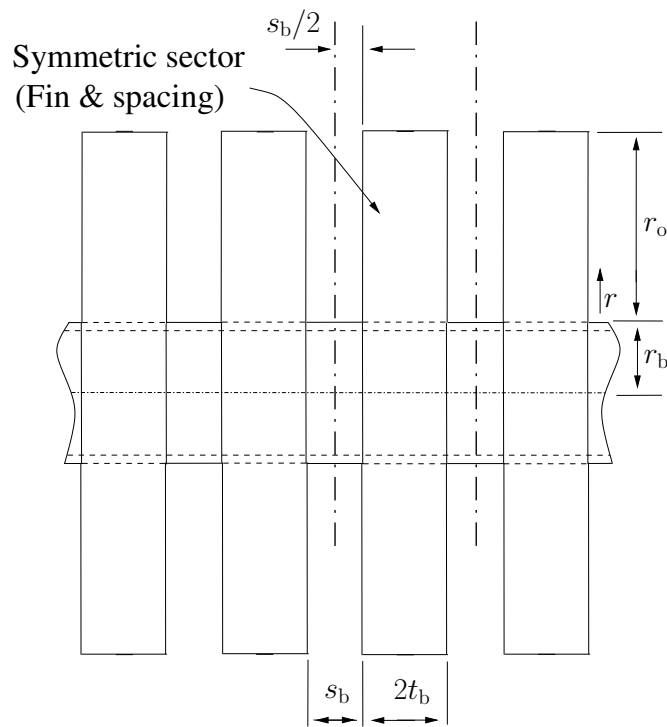
Figure 4.17: Schematic diagrams of annular fin arrays with fins of uniform thickness.

the inner and outer surfaces of each fin being r_b and r_o respectively. The cross-sectional half-thickness of uniform thickness fin is represented by $t(= t_b = t_o)$. On the other hand, s_b is the inter-spacing of the fins (i.e., the gap between two adjacent fins) at the base.

4.4.1 Common formulation for heat transfer equation

The formulation for heat transfer equation of annular stepped fin array and non-linearly varying thickness fin array is already discussed in Section 4.1.1 and Section 4.3.1 respectively. For uniform thickness fin array, $t' = 0$ in Eq. (4.11).

4.4.2 Common Optimization modeling

In the present study the performance of the considered annular fin arrays will be studied in various combination of the considered three objective functions, which for each fin array are the total heat transfer rate $(f_1(\boldsymbol{x}))$, total fin volume $(f_2(\boldsymbol{x}))$ and surface efficiency $(f_3(\boldsymbol{x}))$. The overall thermal performance of a fin array will be enhanced upon maximizing the heat transfer rate and surface efficiency, while the fin material cost will be reduced upon minimizing fin volume. Accordingly, a general multi-objective optimization problem can be formulated for simultaneously optimizing these objective functions.

4.4.2.1 Stepped fin array

The stepped fin array as shown in Fig. 4.1(a) is defined in terms of five parameters. Out of that, four parameters are related to individual fin, which are the radius at the point of step change in thickness (r_1), outer radius (r_o), cross-sectional half thickness of the thick (first) step (t_1) and cross-sectional half thickness of the thin (second) step (t_2). The fifth parameter is the number of fins (n_{fin}) in the fin array. Considering these five parameters as the design variables, the optimization model of the stepped

fin array can be as given by Eq. (4.22).

$$
\left.\begin{array}{rrcl}
\text{Determine} & \boldsymbol{x} & \equiv & (r_1, r_o, t_1, t_2, n_{\text{fin}})^{\text{T}} \\[4pt]
\text{to maximize} & \boldsymbol{z}(\boldsymbol{x}) & \equiv & \{f_1(\boldsymbol{x}), f_3(\boldsymbol{x})\} \\[4pt]
\text{minimize} & \boldsymbol{f}(\boldsymbol{x}) & \equiv & \{f_2(\boldsymbol{x})\} \\[4pt]
\text{subject to} & g_1(\boldsymbol{x}) & \equiv & r_1 > r_{\text{b}} \\[4pt]
& g_2(\boldsymbol{x}) & \equiv & r_o > r_1 \\[4pt]
& g_3(\boldsymbol{x}) & \equiv & t_1 \leqslant \frac{W}{4} \\[4pt]
& g_4(\boldsymbol{x}) & \equiv & t_1 > t_2 \\[4pt]
& g_5(\boldsymbol{x}) & \equiv & \left\lceil \frac{W}{2t_1 + s_{\max}} \right\rceil \leqslant n_{\text{fin}} \leqslant \left\lfloor \frac{W}{2t_1 + s_{\min}} \right\rfloor \\[6pt]
& & & r_1, r_o, t_1, t_2 \geq 0 \ .
\end{array}\right\} \tag{4.22}
$$

In Eq. (4.22), constraints $g_1(\boldsymbol{x})$, $g_2(\boldsymbol{x})$ and $g_4(\boldsymbol{x})$ are related to the geometry of the individual fins, while constraints $g_3(\boldsymbol{x})$ and $g_5(\boldsymbol{x})$ are related to the configuration of the fin array. Constraint $g_1(\boldsymbol{x})$ ensures the existence of the fins by making the radius at step change in thickness (r_1) greater than the predefined radius at the base (r_{b}), and constraint $g_2(\boldsymbol{x})$ ensures the existence of two steps in a fin by making the outer radius (r_o) greater than radius at step change in thickness (r_1) while constraint $g_4(\boldsymbol{x})$ ensures that the inner step of the fin is thicker than its outer step. On the other hand, constraint $g_3(\boldsymbol{x})$ restricts the fin half-thickness at the base (t_1) to such a value that an array of fins can be formed by accommodating at least two fins within the limited predefined length (W) of the primary surface, and constraint $g_5(\boldsymbol{x})$ forms the fin array with the lower limit for two fins and the upper limit avoiding the excess number of fins over the length (W) of the primary surface (($s_{\min}, s_{\max}$) is the allowable range of fin inter-spacing at base). The last line in Eq. (4.22) makes the design variable non-negative.

4.4.2.2 Non-linearly varying and uniform thickness fin arrays

The profile of the non-linearly varying thickness fin, as shown in Fig. 4.12(a), is represented here by a B-spline curve that can be defined by some control points.

Considering that the B-spline curve is defined by m number of control points, their coordinated $P_i(x_i, y_i)$ ($i = 1$ to m) are taken as the design variables, where the x values will represent the radial distances from the base of a fin and the corresponding y values will represent the half-thickness of the fin. In the same way, the uniform thickness fin profile, as shown in Fig. 4.17, can be represented by a single point $P_1 = (x, y)$, where x and y will represent respectively the outer radius and half-thickness of the fin. Accordingly, optimization of both fin profiles (non-linearly varying and uniform thickness) can be modeled by a common formulation as given in Eq. (4.23).

$$
\left.
\begin{aligned}
\text{Determine} \qquad & \boldsymbol{x} \;\equiv\; (n_{\text{fin}}, P_i(x_i, y_i) | P_i(x_i, y_i) \;;\; i = 1 \text{ to } m)^{\text{T}} \\
\text{to maximize} \qquad & \boldsymbol{z}(\boldsymbol{x}) \;\equiv\; \{f_1(\boldsymbol{x}), f_3(\boldsymbol{x})\} \\
\text{minimize} \qquad & \boldsymbol{f}(\boldsymbol{x}) \;\equiv\; \{f_2(\boldsymbol{x})\} \\
\text{subject to} \qquad & g_1(\boldsymbol{x}) \;\equiv\; x_1 < x_2 \leqslant \cdots \leqslant x_m \\
& g_2(\boldsymbol{x}) \;\equiv\; \tfrac{W}{4} \geqslant y_1 \geqslant y_2 \geqslant \cdots \geqslant y_m \\
& g_3(\boldsymbol{x}) \;\equiv\; \left\lceil \tfrac{W}{2y_1 + s_{\max}} \right\rceil \leqslant n_{\text{fin}} \leqslant \left\lfloor \tfrac{W}{2y_1 + s_{\min}} \right\rfloor \\
& s_{\max}, s_{\min} \geqslant 0 \;.
\end{aligned}
\right\} \tag{4.23}
$$

In Eq. (4.23), $P_i = (x_i, y_i)$ is the ith control point and m is the total number of control points of the B-spline curve defining the profile of individual fins of the fin array. Constraint $g_1(\boldsymbol{x})$ makes the control points of the B-spline curve (i.e., their x-coordinate values) distributed along the radially downward direction of a fin and constraint $g_2(\boldsymbol{x})$ ensures that their corresponding y-coordinate values are non-increasing, where $x_1 = r_b$, $y_1 = t_b$, $x_m = r_o$ and $y_m = t_o$ as considered in the schematic diagram of the fin array configuration shown in Fig. 4.12(a). In constraint $g_2(\boldsymbol{x})$, the upper limit of y_1 (i.e., $y_1 \leqslant \frac{W}{4}$) restricts the half thickness of the individual fins at the base (t_b) to such a value that fin array can be formed by accommodating a minimum of two fins within the limited predefined length (W) of the primary surface (in practice, $y_1 \ll \frac{W}{4}$ if the heat transfer from the fins is to be studied as one-dimensional). Since a sharp thickness at the edge of a fin may pose safety hazard, the value of y_m may also be restricted to a finite value within a reasonable

range as widely practiced in real-life applications. Finally, constraint $g_3(\boldsymbol{x})$ ensures the existence of an fin array by setting the lower limit of the number of fins to be two and the upper limit to such a value to avoid the excess number of fins over the length (W) of the primary surface. The range of fin inter-spacing at the base, $(s_{\min}, s_{\max})$, is to be chosen in constraint $g_3(\boldsymbol{x})$ in such a way that Ra remains within the laminar range (see Eq. (4.1)).

For the uniform thickness (rectangular) fin array, $m = 1$ in Eq. (4.23), indicating a single design point,$P_1 = (x_1, y_1)$ as stated above. Here, x_1 and y_1 represents respectively the outer radius and half-thickness of the fin. Note that constraints $g_1(\boldsymbol{x})$ and $g_2(\boldsymbol{x})$ are not applicable in the case of the uniform thickness fin array

4.4.2.3   Formulation of objective functions

In terms of the notations and formulations of heat transfer equation of the fin arrays as presented in Section 4.4.1, the three objective functions in Eqs. (4.22) and (4.23), $f_1(\boldsymbol{x})$–$f_3(\boldsymbol{x})$, can be expressed by Eq. (4.24).

$$f_1(\boldsymbol{x}) = n_{\text{fin}} \times \left\{ -kA_b \left. \frac{dT_i}{dr} \right|_{r=r_b} + hA_{\text{sp}} \left(T_b - T_\infty \right) \right\} \tag{4.24a}$$

$$f_2(\boldsymbol{x}) = \begin{cases} n_{\text{fin}} \times 2\pi \left\{ t_1 \left(r_1^2 - r_b^2 \right) + t_2 \left(r_o^2 - r_1^2 \right) \right\} \; ; \quad \text{for step fins.} \\[2mm] n_{\text{fin}} \times \frac{4}{3}\pi \sum_{n=2,\,4,\,\ldots}^{N} r_{n-1} \left(r_n - r_{n-1} \right) \\[1mm] \times \left(t_{n-2} + 4\,t_{n-1} + t_n \right) \; ; \quad \text{for non-linearly varying thickness fins} \\[2mm] n_{\text{fin}} \times 2\pi t_b \left(r_o^2 - r_b^2 \right) \; ; \quad \text{for uniform thickness fins} \end{cases}$$

$$\tag{4.24b}$$

$$f_3(\boldsymbol{x}) = \frac{1}{n_{\text{fin}}} \times \frac{f_1(\boldsymbol{x})}{hA_s \left(T_b - T_\infty \right) + hA_{\text{sp}} \left(T_b - T_\infty \right)} \tag{4.24c}$$

where, $\quad A_{\mathrm{sp}} = 2\pi r_b s_b$ (4.24d)

$$A_b = \begin{cases} 4\pi r_b t_1 \ ; & \text{for step fin.} \\ \\ 4\pi r_b t_b \ ; & \text{for non-linearly varying and uniform thickness fins} \end{cases}$$

(4.24e)

$$A_s = \begin{cases} 2\pi \left(r_o^2 - r_b^2\right) + 4\pi \left\{r_1 \left(t_1 - t_2\right) + r_o t_2\right\} \ ; & \text{for step fins.} \\ \\ 4\pi r_o t_o + 2\pi \sum_{n=1}^{N} \left(r_n + r_{n-1}\right) \times \\ \left\{\left(r_n - r_{n-1}\right)^2 + \left(t_{n-1} - t_n\right)^2\right\}^{\frac{1}{2}} \ ; & \text{for non-linearly varying thickness fins} \\ \\ 2\pi \left(r_o^2 - r_b^2\right) + 4\pi r_o t_b \ ; & \text{for uniform thickness fins} \end{cases}$$

(4.24f)

A_b in Eq. (4.24a) is the base area of the fin. In Eqs. (4.24b) and (4.24f), n and N are respectively the grid index of space and total number of grid.

4.4.3 Solution procedure

The fin design problem formulated by Eqs. (4.22) and (4.23) as a multi-objective optimization model is solved using the non-dominated sorting genetic algorithm II (NSGA-II).

In the cycles of NSGA-II, the total heat transfer rate $f_1(\boldsymbol{x})$ is computed using Eqs. (4.5) and (4.6) for the stepped fin array, while using Eqs. (4.14) and (4.15) for the non-linearly varying and uniform thickness fin arrays as discussed in Sections 4.1.3 and 4.3.4 respectively.

4.4.4 Numerical experimentation and discussion

In the present study, annular fin arrays with individual fins of various profiles, namely step change in thickness, non-linearly varying thickness, and uniform thickness, are analyzed under the assumptions that the temperature at the base of the fins

is constant, thermal conductivity for the fin material is variable, and heat dissipation from the surface of fin array surface by natural convection only.

The operating conditions and thermal properties of the fin material as well as the fin array geometry with reference to Fig. 4.1(a), 4.12(a) and 4.17 considered here for numerical experimentation, are given in Table 4.4. The user-defined algorithmic

Table 4.4: Operating conditions, material properties, and fin array geometry for annular fin arrays.

Parameter	Value/range of value
Ambient temperature, T_∞	300 K
Temperature of the fin at the base, T_b	373 K
Thermal conductivity of the fin material at T_∞, k_a	186 W/mK
Parameter for variable thermal conductivity, β	-0.00018 K^{-1}
Base radius of fins, r_b	2.0 cm
Outer radius of fins, r_o	2.5–6.0 cm
Fin half-thickness, t (for uniform/non-linearly varying thickness fin)	0.01–0.2 cm
Radius of step change in thickness, r_1 (for step fin)	2.5–6.0 cm
Half thickness of the first step, t_1 (for step fin)	0.01–0.2 cm
Half thickness of the second step, t_2 (for step fin)	0.01–0.2 cm
Length of the primary cylinder, W	40.0 cm
Fin inter-spacing at base, s_b	[0.36, 18.0] cm

parameter settings for NSGA-II are given in Table 3.3. A cubic curves with open uniform knot vector and of order 4 is considered for the B-spline curve to represent the profile of the non-linearly varying thickness fins. Accordingly, the B-Spline curve is defined here by five control points (i.e., for non-linearly varying thickness fins, $m = 5$ in Eq. (4.23)).

Using the above input information and randomly generated NSGA-II population, the fin array design problem formulated in Eq. (4.23) is studied under different combinations of the three objective functions, f_1–f_3, given by Eq. (4.24).

Fig. 4.18 shows the Pareto fronts for the three fin array configurations obtained by maximizing the total heat transfer rate (f_1) and minimizing total fin volume (f_2) of each fin array. The conflicting nature between the heat transfer rate and fin volume is clearly visible. It is also seen that the heat dissipation rate from all the fin arrays are almost same at low fin volume. However, at higher fin volume, the non-linearly varying thickness fin array has a better performance than those of the other two fin arrays, followed by stepped fin array. Nine selective efficient fin array
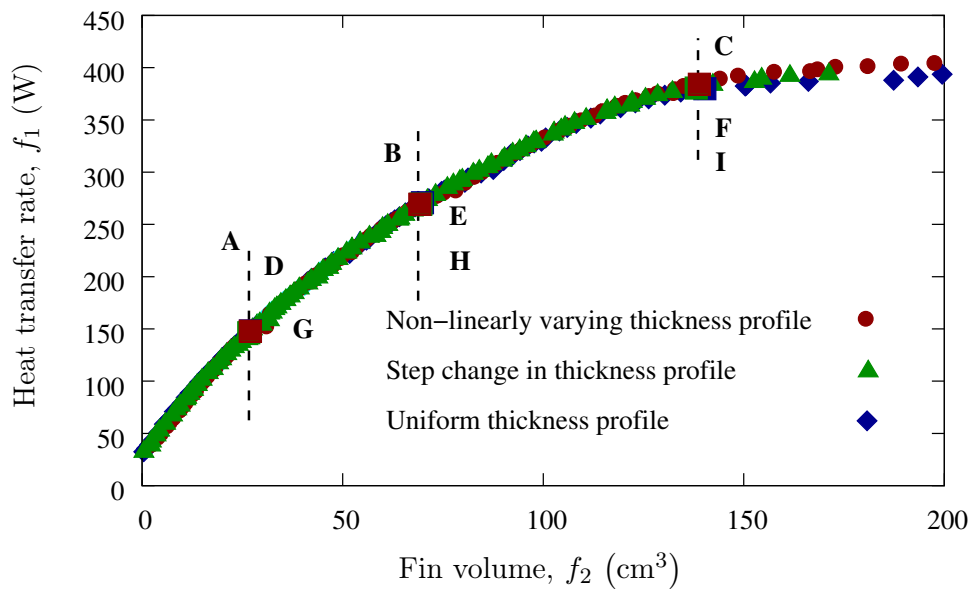
Figure 4.18: Pareto fronts in terms of f_1 and f_2.

configurations corresponding to solutions A–I of Fig. 4.18 (three configurations from each category of fin arrays) are shown in Fig. 4.19, where it is seen that all the fin
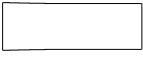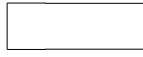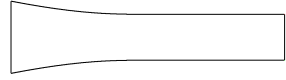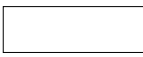

A			B			C		
$f_1 = 147.81$ W	$f_3 = 0.94$		$f_1 = 269.36$ W	$f_3 = 0.87$		$f_1 = 384.22$ W	$f_3 = 0.85$	
$f_2 = 26.97$ cm^3	$n_{\text{fin}} = 35$		$f_2 = 69.22$ cm^3	$n_{\text{fin}} = 48$		$f_2 = 138.91$ cm^3	$n_{\text{fin}} = 66$	
D			E			F		
$f_1 = 146.30$ W	$f_3 = 0.93$		$f_1 = 269.52$ W	$f_3 = 0.84$		$f_1 = 380.54$ W	$f_3 = 0.85$	
$f_2 = 26.61$ cm^3	$n_{\text{fin}} = 31$		$f_2 = 69.51$ cm^3	$n_{\text{fin}} = 43$		$f_2 = 138.15$ cm^3	$n_{\text{fin}} = 68$	
G			H			I		
$f_1 = 148.06$ W	$f_3 = 0.95$		$f_1 = 270.68$ W	$f_3 = 0.87$		$f_1 = 379.88$ W	$f_3 = 0.83$	
$f_2 = 27.02$ cm^3	$n_{\text{fin}} = 39$		$f_2 = 69.90$ cm^3	$n_{\text{fin}} = 49$		$f_2 = 140.31$ cm^3	$n_{\text{fin}} = 70$	

Figure 4.19: Selective efficient fin array configurations corresponding to solutions A–I of Fig. 4.18 (a larger scale in the direction of thickness is used to make the variation prominent in that direction).

profiles at low fin volume tend to acquire rectangular shape, while they become significantly different at higher fin volume. The values of the third objective (f_3)

for those configurations are also computed and shown in Fig. 4.19.

For further assessment of performance, the fin arrays are studied in the second step for simultaneously maximizing the heat transfer rate (f_1) and surface efficiency (f_3). The obtained Pareto fronts are shown in Fig. 4.20, where the heat
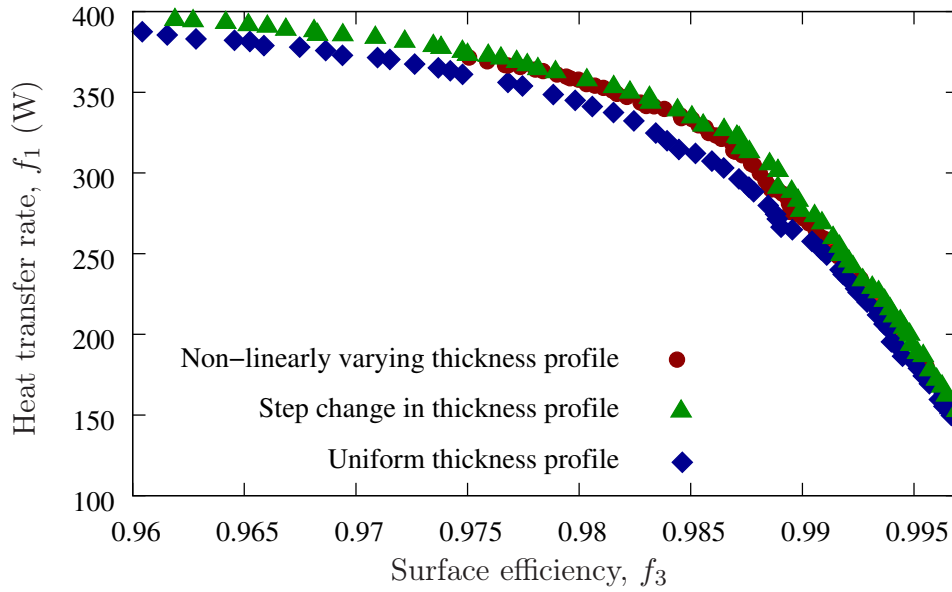

Figure 4.20: Pareto fronts in terms of f_1 and f_3.

transfer rate and surface efficiency are found conflicting with each other. It is also seen in Fig. 4.20 that the uniform thickness fin array configuration has the lowest surface efficiency for similar heat transfer rate among the three fin array configurations whereas the Pareto fronts of the other two fin arrays overlap with each other, indicating almost the same surface efficiency in both the cases.